



POLITECNICO DI MILANO
DEPARTMENT of Electrical Engineering
MASTERS PROGRAMME IN ELECTRICAL ENGINEERING

Test Bench for the Measurement of Electric Field Homogeneity in Electrostatic Separators

Masters Dissertation of:
Muhammad Khurram Shahzad

Supervisor:
Prof. Alessandro Ferrero

CERN Supervisor:
Nicolas Magnin

The Chair of the Doctoral Program:
Prof. Alberto Berizzi

2017 – Cycle

Abstract

Particle accelerators use beam deflectors based on strong Electric Field

deflection, for instance in the new antiproton storage ring ELENA (Extra Low Energy Antiproton Ring) at CERN. During the design, the electric field in the aperture of these deflectors is simulated, but we need a method to measure this field produced on deflectors to validate their correct functioning before using them in accelerators. The report describes the evaluation of techniques to measure the electric field homogeneity in the deflectors, as well as the development of a test bench to automate the measurement principle and its validation for static or pulsed electric field deflectors.

Electrostatic separators when used for beam applications can cause large distortions and undesired bending or collisions of the beam particles with the accelerator body or with the deflector plates. If such a problem arises then it takes lot of effort both in terms of money and labor to fix those sites where the beam has struck. This can sometimes cause irreparable damages as well.

For magnetic deflectors, there are already techniques exist which can provide quite accurate measurements about the axis of the magnets and the regions of field homogeneity. However, there has not been much emphasis done for the electric field measurements and the evaluation of its homogeneity. Current methods exist mostly for some industrial applications but they cannot be safely employed for the deflectors used in accelerators.

Electric field homogeneity lies mostly in the design, dimensions and the fabrication of the separator. Most of the existing techniques consist of simulating the design with Finite element simulators which provides the result equivalent to the actual test environment for which the deflector is designed.

In this thesis, we are going to apply one of the techniques based on voltage measurements and then see the results that can explain how we can control the quality of electrical field by exhibiting its homogeneity.

Summary

T

hesis has been divided into 8 chapters:

Chapter 1 talks about the introduction of CERN, some history, what kind of accelerators are there and what techniques are there being used for beam deflections.

Chapter 2 focuses on the measurement principles of electric field, the instruments currently used to measure the field intensity for various applications, their practicality and drawbacks. Also, it explains the method used in this thesis for the measurement which is based on 2 research papers from 90s.

Chapter 3 introduces the Fast-Coupled deflector designed for the test bench as an initial measurement electrostatic separator. It also focuses on the modeling of the deflector and creating its simulation model. Moreover, it talks about the issues regarding the measurement of very low capacitances.

Chapter 4 explains the design of the circuits for the spice simulation, different circuit approaches and their problems.

Chapter 5 introduces FEM modelling and simulation of electric field in COMSOL for the given models. This simulation sets up the base and reference of how the field homogeneity will look like for a deflector design and how much sensitive is the design for it.

Chapter 6 introduces some basic hardware requirements and the reason of their selection for the test bench.

Chapter 7 throws light on the final hardware design of the test bench, the adjustments in the design and setup.

Chapter 8 shows the final measurement test bench setup, software algorithm, results, improvements and suggestions for future.

III

Contents

1. Introduction	13
1.1 CERN.....	13
1.2 Particle Acceleration.....	14
1.3 Particle Detectors.....	15
1.4 ELENA.....	17
1.4.1 Magnetic Extraction	18
1.4.2 Electric Field Extraction Concept and design	19
2. Electric Field Measurement.....	21
2.1 Basics	21
2.2 Existing measurement tools	22
2.2.1 Magnetic Extraction	23
2.3 Measurement method based on stretched wire	24
3. Fast Coupled Deflector	31
3.1 Specifications.....	31
3.2 Modeling of the deflector.....	33

4. Circuit Simulations.....	37
4.1 Models Proposed	37
4.1.1 First Approach.....	37
4.1.2 Second Approach.....	40
4.1.3 Third Approach.....	43
5. Electric Field Simulations.....	44
5.1 Physics Involved.....	44
5.2 Deflector Model.....	45
5.3 Parallel Plate Model.....	48
5.4 Tilted Plate Model.....	49
6. Hardware selection	53
6.1 Measurement electronics.....	53
6.1.1 PXIe 1071 crate.....	53
6.1.2 PXIe 8100	55
6.1.3 PXIe 4081	57
6.1.4 PXIe 5402.....	59
7. Final Design of the test bench	60
7.1 Remodeling of the circuit used	60
7.1.1 Keithley 6221	60
7.2 Grounded measurement model.....	61
7.2.1 Keithley 2000	63
7.3 Final simulation model.....	63
7.4 Synchronization of generators	67
7.5 Hardware for the wire movement	68
8. Implementation and results.....	69
8.1 Scripting for drivers	69
8.2 Analysis in MATLAB.....	72
8.3 Final images of the setup before the first measurement	75

8.4 Functioning of the test bench.....	77
8.5 Conclusion	83
8.5.1 Possible errors	83
8.5.2 Challenges faced.....	84
8.5.3 Future Recommendations	84
References.....	85

Acknowledgement

The work presented in this thesis was carried out at CERN in the beams department for their technical electronics section (TE-ABT-EC). While working as a technical student for 8 months, I managed to design a test bench for the measurement of electric field homogeneity in beam transfer applications. My work is presented as my Master thesis at my home university Politecnico di Milano.

I will like to thank Nicolas Magnin from Technical Accelerator Beam Transfer Electronics Department (TE-ABT-EC) CERN for providing me the opportunity to work under his great supervision on this thesis. Also, I am very grateful for the support provided by Carlo Petrone and Domenico Caiazza both of (TE-MS-CMM) from the magnetic measurements laboratory at CERN by allowing me work with their existing setups and modifying it for the electric field measurements of the septum and deflectors. I am thankful to Beams Physics department for helping me with the physics simulation. I have been well assisted by Jan Schipper (TE-ABT-EC) and Thierry Paul (TE-ABT-EC) for carrying out work with National Instruments equipment. Afraid of forgetting the names, I will like to acknowledge all the TE-ABT-EC team and the beam physics section for the kind support.

I have enjoyed working with people from different sections and nationalities. I managed to learn a lot from this experience and transformed myself professionally as well as individually.

Moreover, I am honored to have Professor Ferrero Alessandro from Department of Electrical Engineering of Politecnico di Milano as my supervisor for this Master's thesis.

Finally, I want to thank my family, friends and in-particular my parents for all the educational support, freedom and unconditional love; the most precious contribution for my personal development.

CHAPTER 1

Introduction

1.1 CERN

CERN is one of the world biggest research center of Nuclear Physics. It stands for ‘European Council for Nuclear Research’. The foundation of this research center was laid back in 1952 with the focus of research in science and to establish a research center of the Europe. The goal was to lead the European research in physics for understanding the universe. At that time, there were certain theories about the existence of the universe and how to unveil its hidden truths. There was a need of an experimental place where scientists can sit down and try to validate their theories.

Right now, it stands as the biggest hub for engineers and scientists which are working day in and day out to achieve results that can improve our basic understanding of the universe. It provides a common platform for research in experimental physics with the collaboration of the universities worldwide.

LHC is the biggest circular particle accelerator at CERN. It has a circumference of 36 Km. It stands as the largest machine in the world. It is basically a tunnel where particles are being accelerated under the effects of high electric and magnetic fields.

Complex electrical and electronic circuits regulate the experiment. In such experiments, the precision in the measurements and errors play a key role. Since the particles are forced to move and accelerate in circular rings, magnetic and electrostatic deflectors are used to bend the particles in the circular paths or to transfer them from one ring to another one.



Figure. 1 LHC Tunnel [1]

1.2 Particles Acceleration

The particle acceleration is not done directly in LHC. In fact, LHC is the last stage of the acceleration. The process starts from a bottle of hydrogen where strong electrostatic field removes the electrons and creates positive charge particles of hydrogen (called protons). LINAC (Linear Accelerator) is used to accelerate these protons up to the energy of 50 MeV. In this stage, the acceleration path is straight one.

Once the LINAC operation is finished and protons gain the required energy, they are deflected and transferred to the second stage which is the first and smallest circular accelerator. It's called Proton Synchrotron (PS). The goal here is to make the particles circulate until they reach the energy of 1.4 GeV. This increase in energy is provided by the magnetic field since the particles are kicked by the kicker magnets. With every kick, the energy gets boosted. After this stage, the protons are deflected and again transferred to a bigger ring. This is called Super Proton synchrotron. Here the boosting of energy follows the same process as mentioned for PS. But not the protons are accelerated until they reach the energy of 450 GeV. Now they are ready to be transferred to LHC where the energy of these protons is increased up to 6.5 TeV. At this stage, they are moving at the 99.999% speed of light. [1]

There are always two beams of these protons in LHC, this is done when they are transferred to this ring and these protons move in opposite directions until the collisions take place. The figure below gives a clear picture of all the possible paths taken by the particles. Some of the stages named as ISOLDE and AD (Antiproton Decelerator) are the experiments which don't require protons to have high energy therefore depending on the need they are transferred to those facilities from PS.

CERN Accelerator Complex

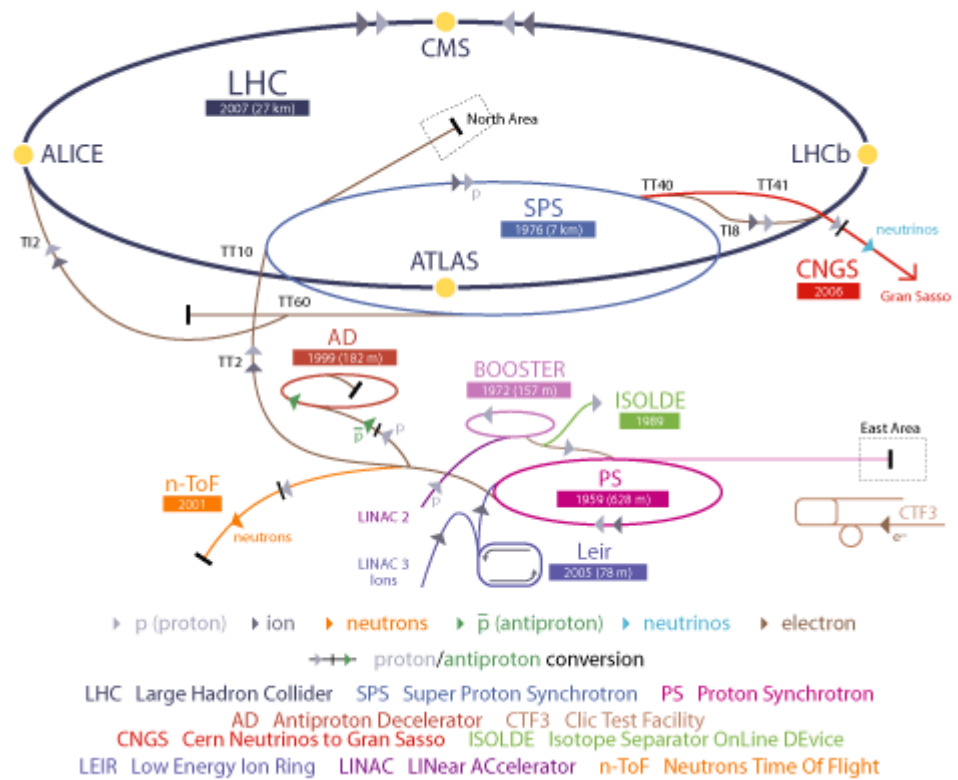


Figure. 2 CERN Accelerator hierarchy [1]

1.3 Particles Detectors

There are 4 collision detectors lying up to the depth of 100 meters down the earth. These are ALICE (A Large Ion Collider Experiment), ATLAS (a place where the discovery of Higgs boson is done), CMS (Compact Muon Solenoid) and LHCb (Large Hadron Collider beauty).

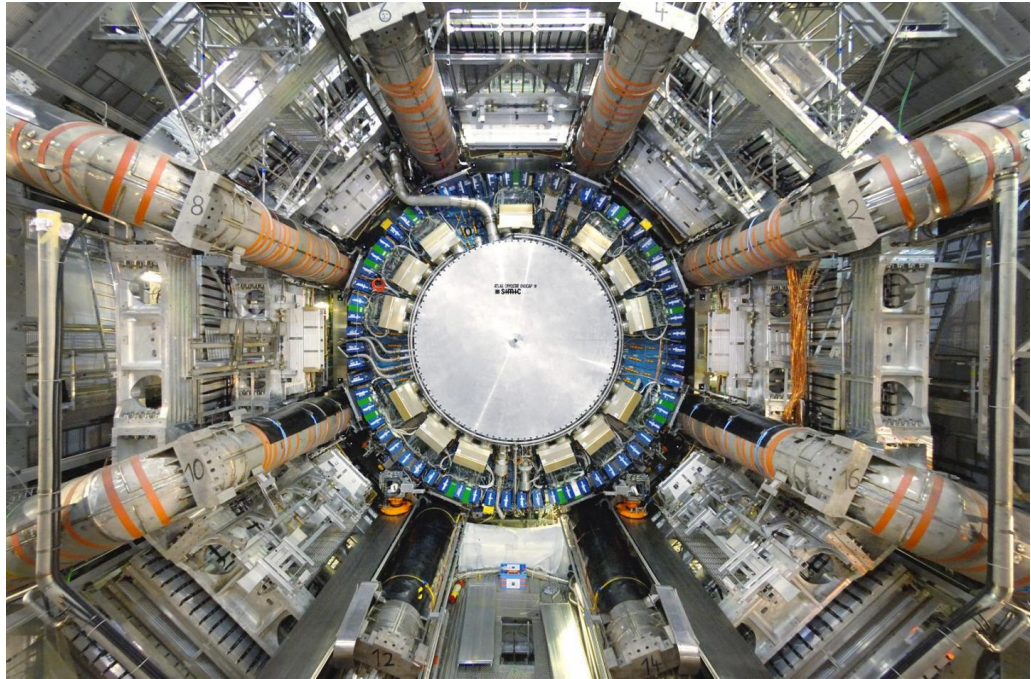


Figure. 3 Atlas detectors [1]

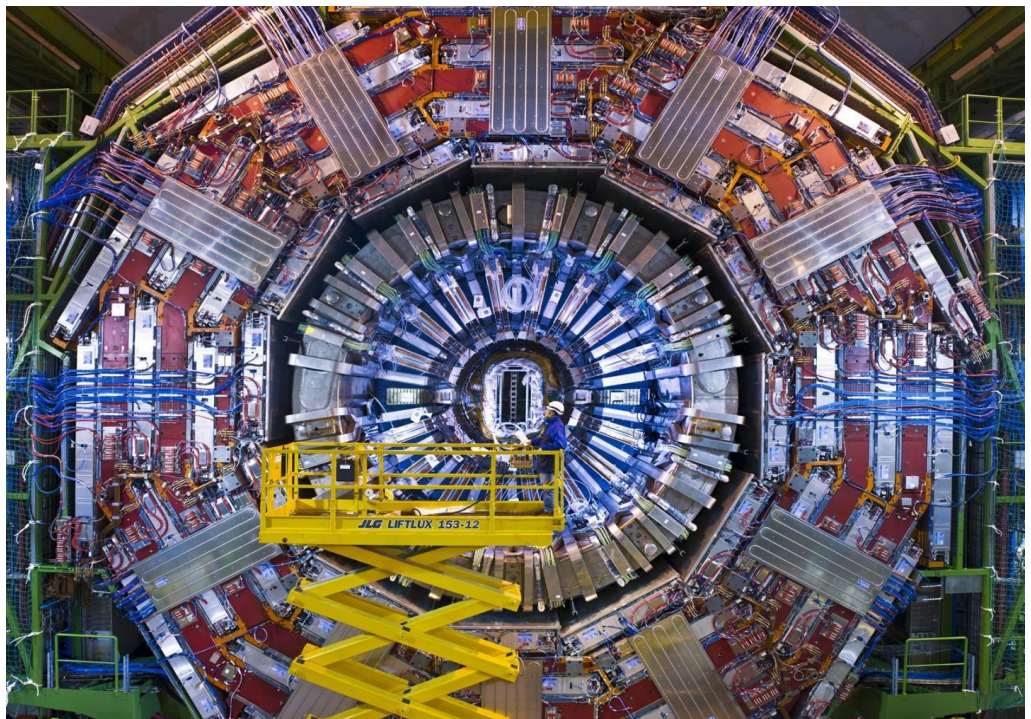


Figure. 4 CMS detector [1]

1.4 ELENA

ELENA project started in 2011 and at the start one extraction method of beam was proposed with the help of magnetic septum's and kickers. Alternatively, a second proposal was to use electrostatic deflectors to achieve the same operation.

ELENA (Extra Low Energy Antiproton Ring) is a decelerating ring where antiprotons are slowed down from 5.3 MeV to 100 keV. The idea is to slow down these antiprotons to perform experiments on them such as spectroscopy and most importantly to study the effects of gravity on antimatter. Since they are not the matter which is attracted by the gravity. The impact of gravity on these particles will likely to reveal different effects. The accelerators beams are transferred using deflectors.

One of the deflector designed for ELENA is called Fast Pulsed Deflector. It is based on the proposal to use electric field for injection, extraction and transfer of the beam. For the design of the deflector, its power, the pulse width, pulse timings and the electric field which it will generate are taken into consideration.

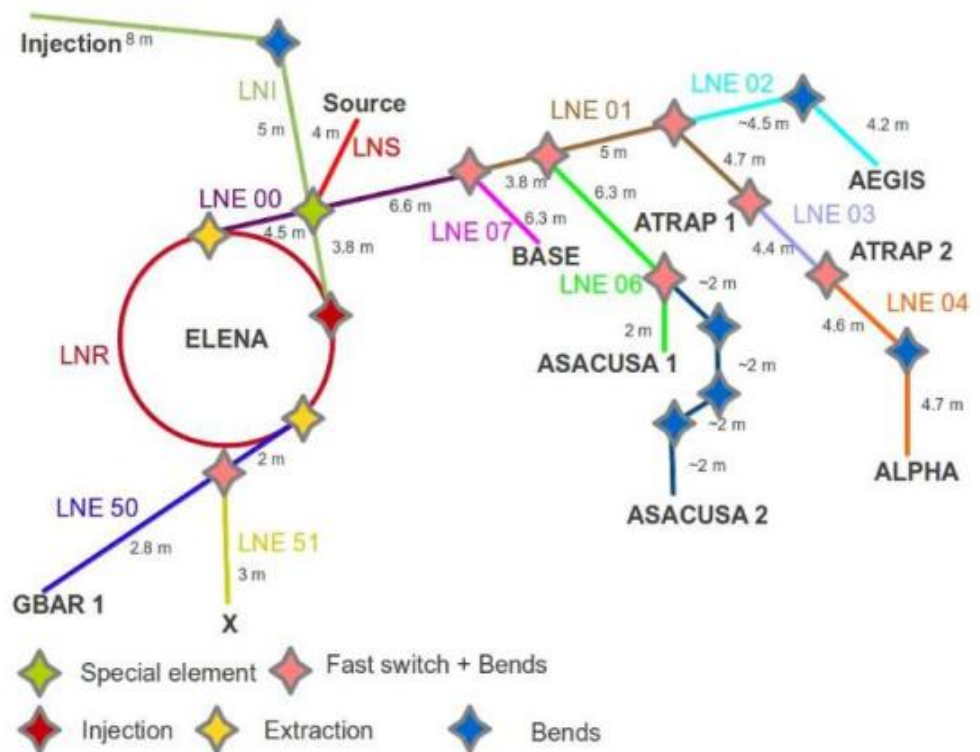


Figure. 6 ELENA extraction [2]

The above figure explains the points of injection, extraction and transfer of beams for ELENA.

1.4.1 Magnetic extraction

The concept of magnetic extraction comes from the basic equation of force on a charged particle in the presence of magnetic field.

$$F = q. (v \times B) \quad (1)$$

This force is directional and depends on the cross product of the velocity of the charged particle and magnetic field through which it is passing. Therefore, based on this principle the magnetic kickers were already present and the one used at the start had the following dimensions:

	Injection Septum	Extraction Septum	Extraction kicker
Deflection angle [mrad]	340	392	383
Beam energy [MeV]	5.3	0.1	0.1
$\int B \cdot dl$ [mT.m]	113	18	18
Septum thickness [mm]	22.8	22.8	n.a.
# turns	20	20	1
Current [A]	1120	178	1492
Rise/fall time (2 – 98)% [ns]	DC	DC	200
Flat top length [ns]	DC	DC	0-600

Table .1 Deflector data [3]

The two types of septum and one kicker have their own design characteristics. Injection is the point of entrance in to the septum. The beam energy at the point of injection is very high, consequently the current required to generate enough field to bend the beam is high. Although for extraction, it is lower. For kicker, the time of operation must be fast enough therefore, the current required is very high for short duration just to provide enough kick in very brief time.

Magnetic kicker is designed using C-shape ferrite cores which are interleaved because of high voltage operation. Outside support is made up of stainless steel. It is placed in a vacuum chamber and heated up to 300 degrees Celsius to achieve the desired pressure. The magnet is powered by high voltage converter which contains SF6 and 15 Ω pulse forming line (PFL). Converter

contains thyatron switches and the pulse length is controlled by using these switches. Single extraction can be done at the rate of 1 Hz repetition. Magnetic Septum is very like the kicker design but operates at lower value of the current.



Figure .4 Magnetic Septum Magnet [3]

To design such kickers and Septas, the cost for the manufacturing of magnets is very high. A low-cost solution is to use fast pulsed deflectors based on the principle of electric field.

1.4.2 Electric Field Extraction Concept and design

Electric field produces force on charged particles. In electrostatic or pulsed deflectors, the principle is to deflect the beam by controlling the electric field that will cause the particles to bend to a precise angle. Since the size of the particles is very small therefore to bend their path, the electric field acting on them should be homogeneous to experience a constant force along the trajectory.

$$\mathbf{E} = \frac{\mathbf{F}}{q} \quad (2)$$

The fast deflector is designed to have the electric field homogeneity of ± 0.1 % that can deflect the beam by an angle of 180 mrad. The following parameters show the initial design values:

Good field region	Ø 52	mm
Deflection angle	180	mrad
Physical device length	700	mm
Electrode length	400	mm
Electrode height	130	mm
Electrode gap	115 - 130	mm
Voltage	± 5.1	kV
Deflection angle homogeneity (H)	± 1	%

Table 2. [3]

The resulting geometry of the fast-pulsed deflector is taken as non-parallel orientation to the deflecting beam. Following picture shows the simulation result based on the above construction parameters.

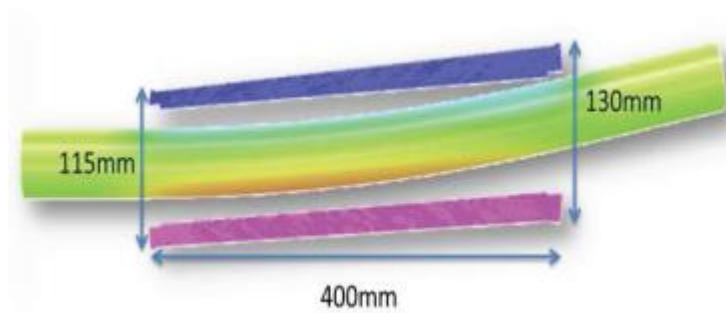


Figure 6. Beam deflection lengths [3]

The next challenge was to design the deflector for the field homogeneity of $\pm 0.1\%$.

CHAPTER 2

Electric field measurement

2.1 Basics

Electric field is produced between the electrostatic deflector plates by static charges that position themselves depending on the dielectric medium used and applied voltage. Although if the charge distribution is known, then by using equation (2) and the expression of Coulomb's law, we can determine the electric field. But the charge distributions are not easy to find because measuring it can distort its uniformity and there is no setup or measuring instrument that can effectively measure it. Another way is to leave a charge in the electric field and measure the force on it but this is again impractical because a complete setup required is not feasible. One of the best ways is to measure it indirectly by relating it with electric potential. In this method, all the uncertainties of the measuring equipment rely on the voltage measurement error mostly. Electric potentials can be measured with a highly precise voltmeter with a high input impedance.

It can be defined as the electrical work performed on a unit charge when the point charge is moved from one point to the other.

$$V = \frac{W}{q} \quad (3)$$

Where electric work can be defined as the force times the distance. It is the dot product of vectoral force and vector distance.

$$W = \mathbf{F} \cdot \mathbf{d} \quad (4)$$

Combining (3) and (4) we can achieve (5)

$$V = F \cdot \frac{d}{q} \quad (5)$$

By using (2) and (5), we rearrange and make the distance to approach zero, we achieve (6).

$$E = - \left(\frac{\partial V}{\partial d} \right) \quad (6)$$

2.2 Existing measurement tools

2.2.1 The electrostatic field meter

As the name implies, this type of tool can be used to measure the field and ideally it should have the capability of measurement of the electric field without distorting it. The field distortion can happen in many ways because of the field produced itself by the measuring equipment as well as the measurement reference should be isolated from the ground. This can be achieved by using floating referenced measurements which are not easy to handle. The concept of floating measurements can be explained by considering the following figure:

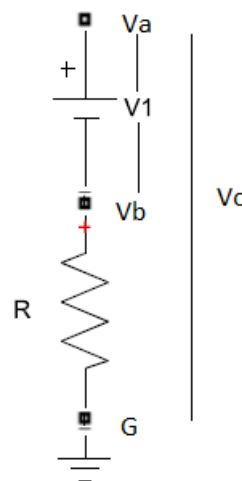


Figure 7.

Above figure shows two terminals which can be used as a reference for the measurement. If we measure everything with respect to ground, then the measurement probes should be set at V_a and G thus measuring the potential difference of value V_c . To measure V_1 , the probes should be placed at the points of V_a and V_b .

As shown in the figure, the point V_b can have a floating potential if the resistor below it has impedance of several mega ohms. Although, it will still not 100% be floating because of a path to the ground.

2.2.2 Types of field meter

Electrometer is a first type which is a small handheld device. It has an amplifier coupled with a shunt capacitor. Ideally the amplifier should not draw any current but in practice it draws some leakage current and that can cause error in the measurement. The current can be determined by tuning the shunt capacitor using the expression below:

$$I = C \frac{dV}{dt} \quad (7)$$

For every measurement, the capacitor must be discharged for a known field before the next measurement. The main advantage of it is its low cost and small size. While the need to zero the charge on the capacitor makes it less practical for precise and automated applications.

Second type makes use of radioactive sensors. Radioactive sensor causes the ionization of the air surrounding it. As soon as the electric field makes a contact with this ionized air, the disturbance generates small current which is measured to obtain the electric field. Its radioactive sensor material and the effect of dirt on the sensor make the use of such field meter to very limited applications.

The previous 2 approaches are based on DC circuits mainly while the third type employs the use of AC signals for the measurements. This is achieved by designing with 2 constructions.

1. First construction contains a small motor whose rotor is crossing the electric field and stator acts as a sensitive electrode. This system is a bit bigger and the response of motor must be controlled which can involve designing a feedback loop system. Also, the speed is limited due to the rate at which the rotor is crossing the E-field. The basic block diagram is shown below:

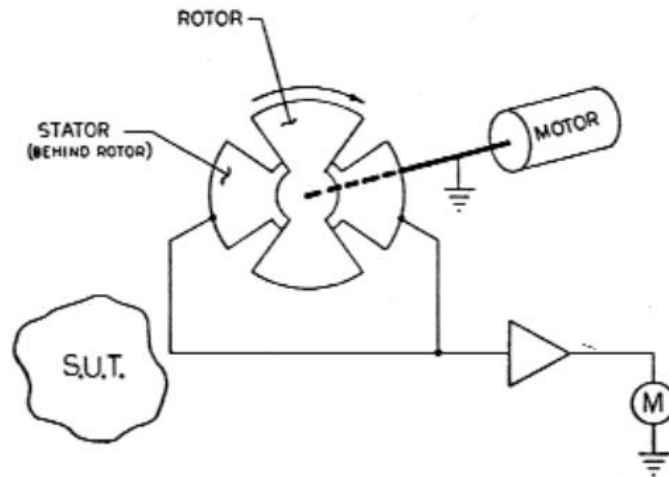


Figure .8 Rotor based meter [4]

2. Second construction involves a capacitor whose plates are vibrating which interact with the existing field to produce induced voltage.

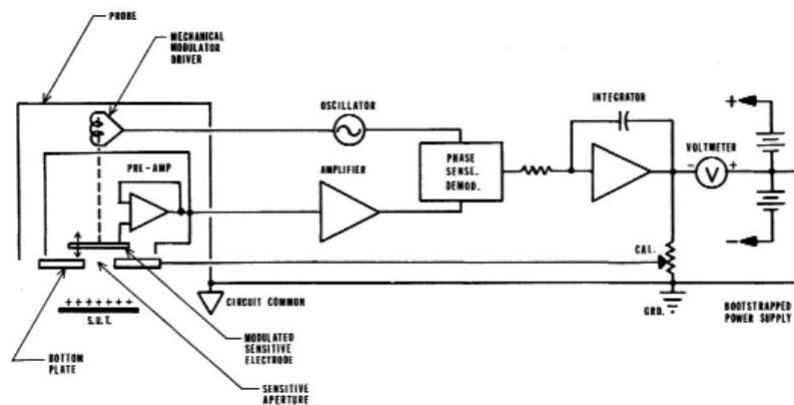


Figure. 9 Capacitor based meter [4]

This induced voltage is then sent to an amplifier which transfers it to a phase sense demodulator. Demodulator sends the phase value to the oscillator which then tried to produce the oscillations to minimize the induced voltage. Meanwhile an integrator continues to integrate the voltage and this is measured by the voltmeter whose one end is fixed at 0 V with dc batteries connected with their grounds made common.

Both above methods yield the uncertainty in measurement of ± 0.01 V/mm. For our application, we require the accuracy of up to 0.0001 V/mm.

2.3 Measurement method based on stretched wire

This method was proposed by Weiran Lou and James J. Welsch at Cornell University United States of America. By using this method, it was proposed that by using very precise measurement tools, the precision in field measurement up to 1 μ V/mm can be achieved.

According to them, we can measure the electric field indirectly by using stretched wire along the trajectory of the beam placed in between the plates of the deflector. Because of it, charge will be induced on the wire which can be reduced to zero by adjusting the potential of the wire with respect to the deflector plates.

The induced charge can also be measured by connecting the wire with an oscilloscope and by applying a time varying electric potential on the plates. For any fixed position of the wire, if we can determine the induced voltage then it can be made zero by moving the wire to some other precise position. This can define the point where the field due to positive plate potential cancels out the negative plate potential.

After defining this point, wire can be moved to other precise locations and the voltage induced on the wire can be measured. Once we have the data of all the induced voltages on the wire with respect to positions then we can use the expression mentioned in the equation (6) to calculate the electric field.

Alternatingly equivalent results can be achieved by first setting the wire potential using a potentiometer to a fixed voltage with respect to one of the electrodes and then the wire is moved to distinct positions until we measure zero flow of current through the wire. According to the research paper, this approach of first fixing the potential of the wire and then moving it until the induced voltage balances out the charge already given to wire produces accurate results.

One of the advantages mentioned about this method is that a very simple setup is required to use this method. It requires the use of a function generator which can generate sinusoidal or square shape waveforms, a single stretched wire, a precise potentiometer, the translation stages to move the wire, very precise voltmeters and a high impedance oscilloscope. The measurement tools accuracy gives the accuracy of the calculated electric field.

One of the assumptions that has been taken is that as the wire is translated in between the 2 electrodes which are excited by time varying voltage, the electric field and the relative potential of the two electrodes with respect to the wire should remain constant. In other words, this stretched wire should not change the electric field which we are required to measure. Obviously, this can never be 100% true but with the simulation of electric field homogeneity in COMSOL we will be able to tell that whether it is affecting the original field or not or at least by what factor does it affect the field.

Then by taking the assumption that during the whole trajectory of the wire translation the field is not changed then the charge induced on the wire can be made equal to zero with respect to the charges on the electrodes.

Consider the electric field generated by electrodes is E' . This is the field that we intend to measure. Now we can take the expression of the electric field generated by charge on a wire with λ is the charge per unit length of the wire and r is the distance from the center of the wire to be following:

$$E_{wire} = \frac{2\lambda}{r} \quad (9)$$

By controlling the voltage on the wire, the charge given to the wire can be controlled. However, when we position the wire near the electrodes then this cannot be said entirely true because the polarization phenomenon will play its role there and will cancel out the field produced due to the electrode. Therefore, there is a threshold region after which our measurements will not make any sense. In case of symmetrical voltages on the plates, the region of measurement for field homogeneity should exist close to the center.

The measurement technique follows by supplying a $\pm V_o$ potential to the electrodes and providing a zero potential to one end of the wire $V_{wire}=0$ V. Now suppose that the wire is moved along x-axis and it's in the xy-plane where z-plane is along the length of the wire. Due to the oscillating electric field between the electrodes and the change in position of wire, charges will be induced which will flow towards the 0 V fixed end. Therefore, wire position is changed to various locations such that the induced current goes to zero. This point which we can call x_o is the point where the net charge on the wire is 0 and this serves as our origin. If the deflector plates are perfectly symmetrical and aligned right in front of each other as well as the voltage supplied on both the plates are completely 180 degrees out of phase then we can easily assume that the origin lies exactly in the middle of the two plates.

Anyhow, by considering the above setup we can deduce the following equations:

$$E = E_w + E_o \quad (9)$$

Where E is the electric field present at any point between the deflector plates which is the sum of the electric field due to the wire and the intrinsic electric field of the plates.

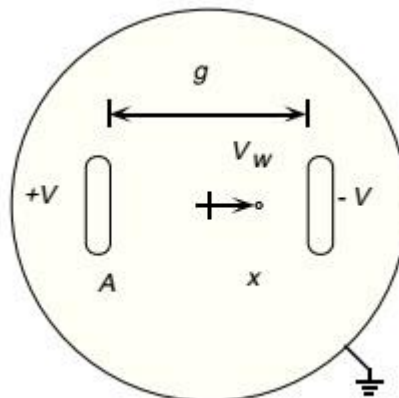


Figure 10. [5]

In figure 10, the point A marks the positive electrode and the gap between the two electrodes is 'g'. The body of the deflector is grounded. If we take ideal scenario with electrodes perfectly symmetrical and aligned, also assuming the voltage applied are also of the same magnitude with 180 degrees out of phase to each other. Therefore, the center point 'g/2' is the point of origin.

Now following on with the figure 10, if we move the wire from point 'A' to 'x' then the following equations are valid:

$$(V_A - V_w) = \int_{(A)}^{(x)} E dl \quad (10)$$

By taking origin as the center and defining it as '0'. The system can be referenced and equation 10 splits up into the following further equations:

$$= \int_{(A)}^{(0)} E_0 dl + \int_{(0)}^{(x)} E_0 dl + \int_{(A-x)}^{(-\phi/2)} \frac{2\lambda}{l} dl \quad (11)$$

But with respect to origin we can say:

$$V_A = \int_{(A)}^{(0)} E_0 dl \quad (12)$$

Now from (11) and (12):

$$-V_w \approx \int_{(0)}^{(x)} E_0 dl + \int_{(A-x)}^{(-\frac{\phi}{2})} \frac{2\lambda}{l} dl \quad (13)$$

At every position of the wire, net charge on the wire is forced to go to 0 therefore λ goes to 0 as well and (13) is reduced to:

$$-V_w \approx \int_{(0)}^{(x)} E_0 dl \quad (14)$$

According to the above resulting equation, the electric field at any position E (x, y) can be defined as:

$$E_0(x, y) = -\nabla V_w \quad (15)$$

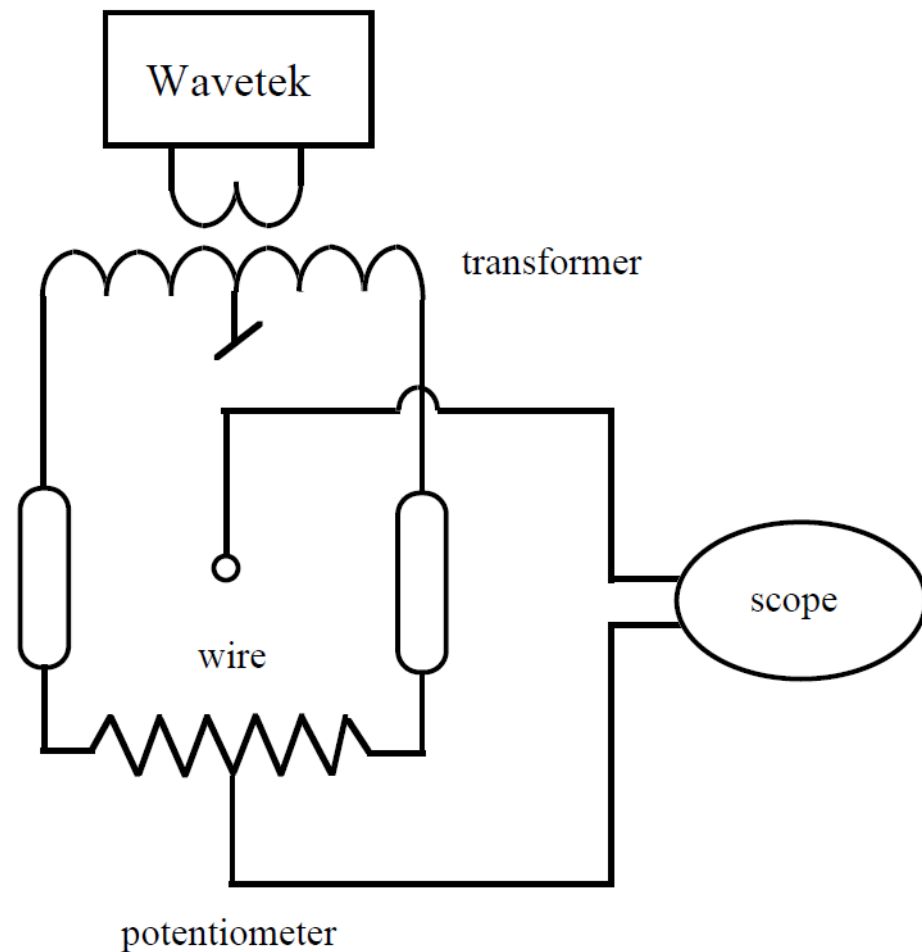


Figure 11. [5]

The figure.11 shows the experimental setup used to carry out the field measurements which is according to the explanation given in the section earlier.

Later, with further developments done by Alexander B. Temnykh and James J. Welch at Wilson Laboratory again at the Cornell University, the setup was improved. Moreover, different sets of experiments were carried out which contained the frequency sweep, amplitude and waveform sweep. But also, they are focused on finding the region where they can define the field homogeneity up to certain error value.

The improved method also involved the elimination of charge induced due the coupling capacitance between the measurement probe and the wire.

The figure in the next page illustrates the final circuit used:

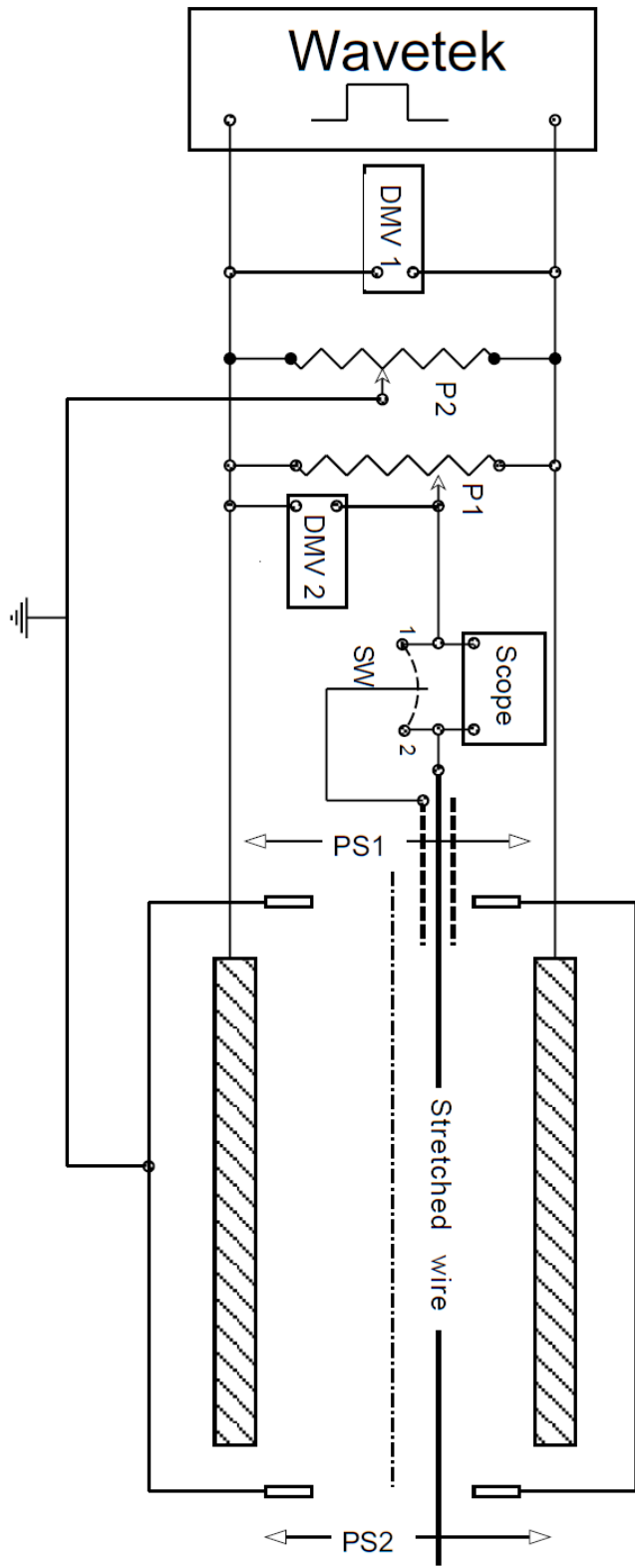


Figure 12. [6]

The setup explained in figure 12. contains information about the electrical instruments used to carry out the measurements. A Wavetek function generator was used to generate sinusoidal and squared wave signals of varying frequencies ranging from 400 to 4000 Hz. After that DMV1 which is an abbreviation of digital multimeter 1 was used to measure the potential difference between the two plates. Two linear stages potentiometer were also employed. Potentiometer P1 is used to balance out the charge induced on the wire by giving the wire end connected to it the same potential as the floating end. Potentiometer P2 served the purpose of keeping the potential on the plates symmetrical and 180 degrees out of phase to each other. This was done by center tapping the P2 to the ground. DMV2 is used to measure the potential of the wire. The scope used had floating terminals for the measurement and had very high input impedance.

The similar approach as mentioned in the figure is used in the thesis with a different type of deflector and in verifying the validity of this method to measure the field homogeneity up to the target precision.

CHAPTER 3

Fast Coupled Deflector

3.1 Specifications

The following image shows the test deflector under test:



Figure 13. Deflector for ELENA

The body of the deflector is made up of Aluminum and has the following specifications:

Beam energy	100	keV
Deflection nominal (max.)	220 (240)	mrad
Required electric field (max.)	0.11 (0.12)	MV/m
Electrode capacitance (w.r.t to virtual ground, without feedthrough)	27	pF
Required Voltage nominal (max.)	± 6.1 (6.7*)	kV
Gap between electrodes upstream	115	mm
Gap between electrodes downstream	130	mm
Electrode height	130	mm
Electrode length	400	mm
Beam acceptance (\emptyset)	60	mm
Field homogeneity (horizontal plane)	± 0.75	%
Good field region (\emptyset)	52	mm
Rise time (0.1 – 99.9%)**	< 1	μ s
Fall time (99.9 – 0.1 %)**	< 1	μ s
Flat top length	0.4 - ∞	μ s
Flat top stability	0.1	%
Device length (flange to flange)	500	mm
Tank diameter	277	mm
Upstream tank flange	DN 273	
Downstream tank flange	DN 273	

Figure 14. Fast Coupled Deflector design [2]

From figure 14, the most useful information that is required for the setup is electrical capacitance which is measured through a simulation with respect to a virtual ground at the center of the deflector. Gap between electrodes upstream and downstream are also important to model the system electrically. Electrode height, length and tank diameter are other useful piece of information. The planar view of the electrodes with its dimensions are shown in the following figure:

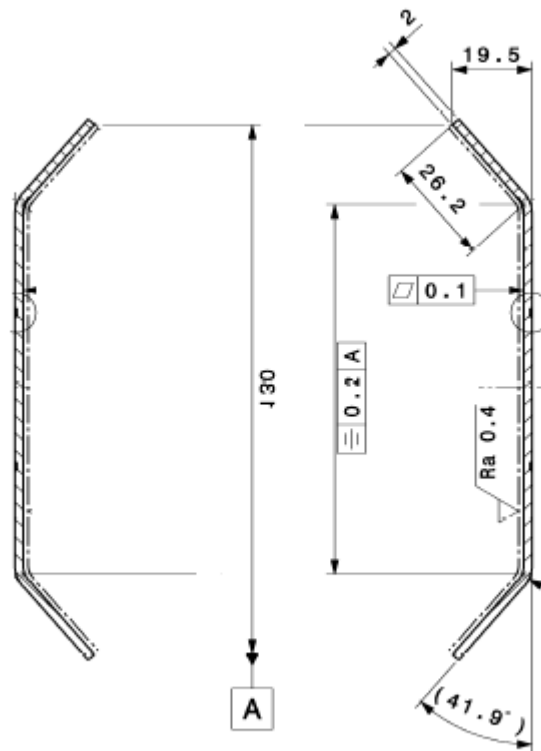


Figure 15. Deflector dimensions [7]

3.2 Modeling of the deflector

The deflector behaves as a capacitor/electrostatic separator with a certain capacitance value. From the basic physics, we know the equation used to calculate the capacitance of 2 parallel plate capacitor is $C = A\epsilon/d$ with 'C' is the capacitance, 'A' is the surface area of the plate, ' ϵ ' is the permittivity constant in air with value of 8.85×10^{-12} (C². N⁻¹.m⁻²) and 'd' is the distance between the plates. As can be seen in the figure 4, the plates are not composed of only two parallel surfaces. The curved ends at the top and bottom are used for field confinement and to minimize the fringing effect of electric field at the ends. By neglecting the top and bottom ends, the geometry simplifies to two parallel plates for which the theoretical calculation leads to the value of 5.75 pF with given dimensions in figure 15.

A highly precise RLC meter FLUKE PM6304 measures the capacitance at different frequencies ranging from 1 kHz to 10 kHz, the measurement averaged out to be 19 ± 0.01 pF for the range specified.

Again, the capacitance of the plates was measured by placing a wire in between the plates and two different measurements were carried out at each position. First, one was

capacitance between first plate and the wire and the second was between wire and the second plate. The following table shows the measurement results.

Distance from positive plate in cm (± 0.10 cm)	C1 in pF (between right electrode and wire) ± 0.01 pF	C2 in pF (between wire and left electrode) ± 0.01 pF
0.50	2.63	6.64
1.00	2.73	5.80
1.50	2.86	5.27
2.00	3.02	4.88
2.50	3.26	4.56
3.00	3.45	4.24
3.50	3.69	4.01
4.00	3.91	3.78
4.50	4.17	3.57
5.00	4.44	3.32
5.50	4.77	3.21
6.00	5.17	3.05
6.50	5.66	2.90
7.00	6.41	2.82
7.50	7.70	2.72

Table 2 — Capacitance measurements

The capacitance values do not appear to be symmetrical. Possible errors in the measurement can be the error in the position that is one mm, the alignment of the deflector plates affect the symmetry as well because they should be parallel (ideally), the tension of the wire (the tension is maintained by putting weights through a pulley and one end of the wire is attached to it initially). The graphs below explain the behavior of these capacitances. Positive plate corresponds to the position 0 cm while the negative one 8 cm.

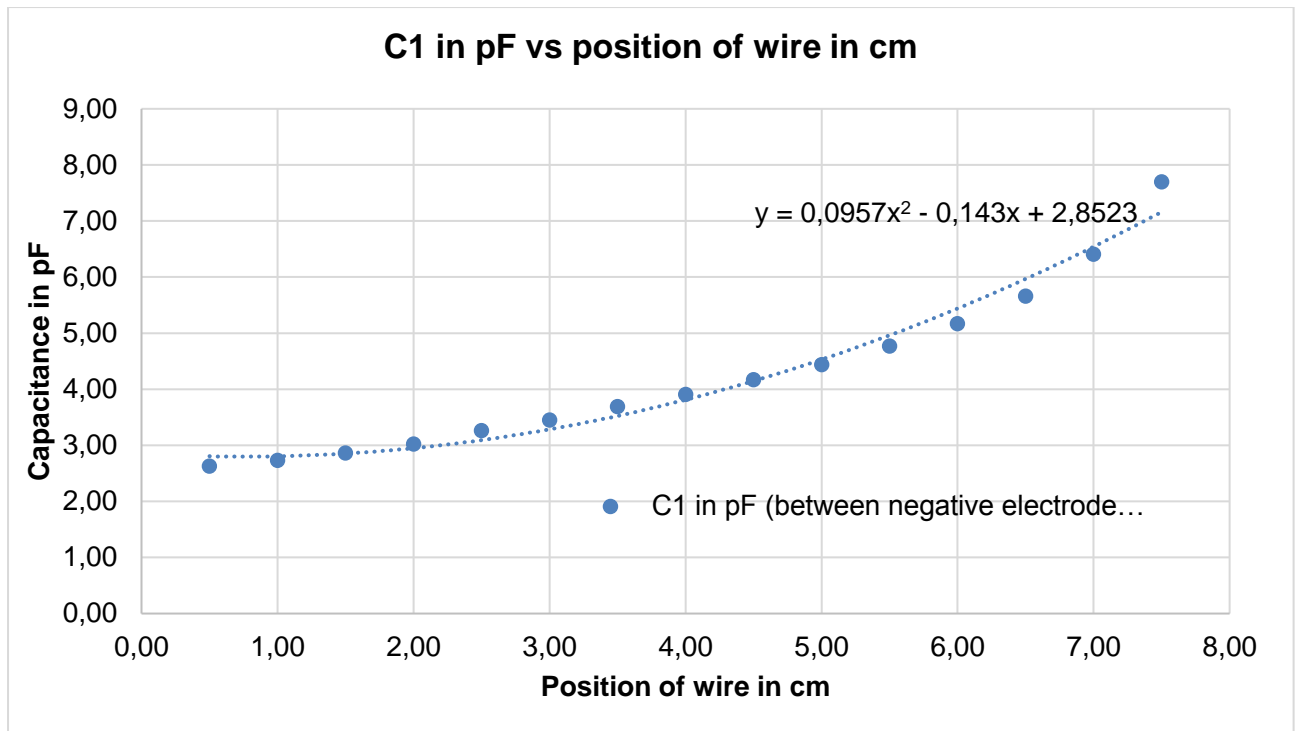


Figure 16 — Capacitance between wire and negative electrode.

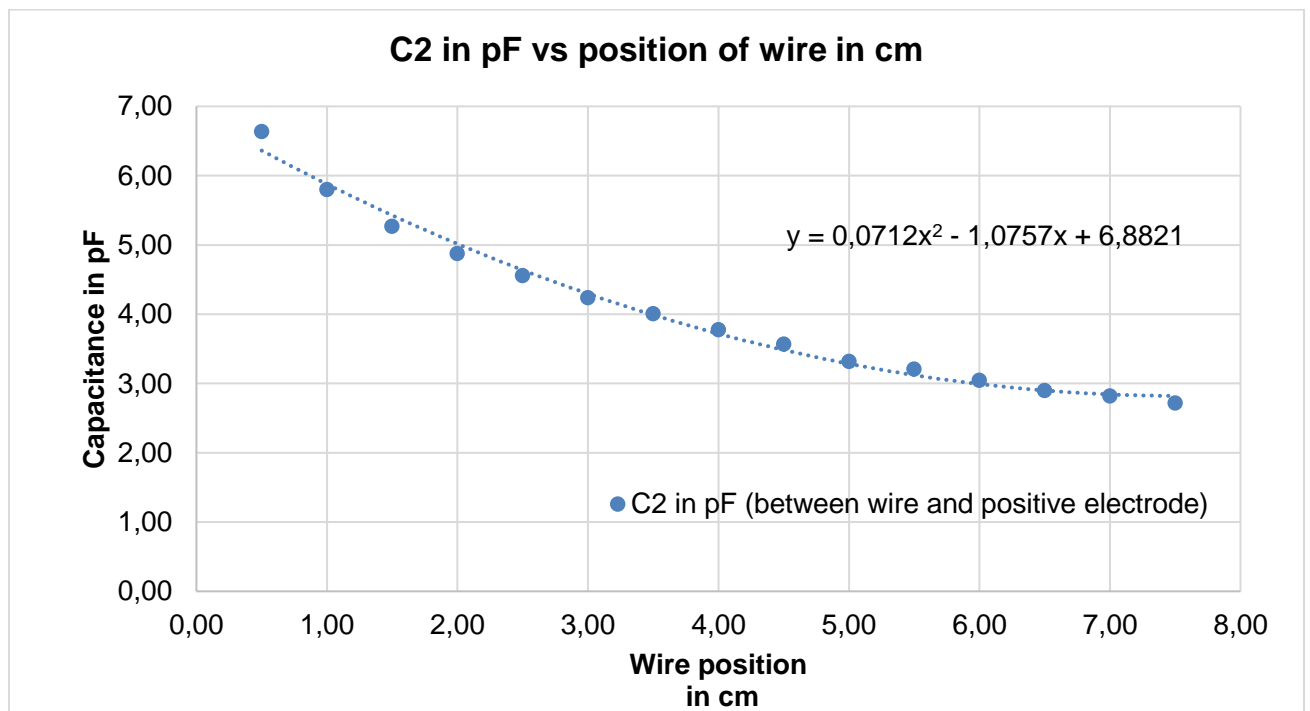


Figure 17 — Capacitance between wire and positive electrode

One of the key points in the measurement of such low capacitance values is to make sure that the measurement instrument has capacitance lower than the value to be measured.

The above set of measurement was taken with the FLUKE instrument as mentioned above and has the input channel capacitance as low as 2 pF. The data from the measurement is used to characterize nonlinear capacitors for the electrical simulations.

The data is also used to fit the curve using a quadratic polynomial fit which is giving the resulting equations each for the change in the value of capacitance between the wire and the respective electrodes. This information can be used to parametrize the capacitors for the electrical spice simulation which is done in the following chapter.

$$C1 = 0.0957x^2 - 0.143x + 2.8523 \quad (16)$$

$$C2 = 0.0712x^2 - 1.0757x + 6.8821 \quad (17)$$

where 'x' is the distance from respective electrode and ranges from 0 to 8 cm. The units of C1 & C2 is pF. The value of C1 when it's close to the negative electrode is around 3 pF when $\lim x \rightarrow 0$, which practically cannot be measured with the instrument employed of taking the measurement because it's almost close to the threshold limit of capacitance measurement. In practice, the measurement can also not be taken at '0' point which means the wire is in contact with the electrode and will no longer should be treated as capacitor.

CHAPTER 4

Circuit Simulations

4.1 Models proposed

In this chapter, the simulation models which are built using the capacitance measurement are discussed. The different models used had certain advantages and disadvantages which are elaborated in the following part of the chapter.

4.1.1 First Approach

Stretched wire in between the deflector plates has been modelled as a capacitor divider with a resistor (wire resistance) connected between the two capacitors C1 (Capacitance between positive plate & wire) and C2 (Capacitance between negative plate & wire). By using the plots from figure 5 and 6, the polynomial curve fit of the data provides respective equations. The independent variable in both cases is the wire position and the dependent is capacitance.

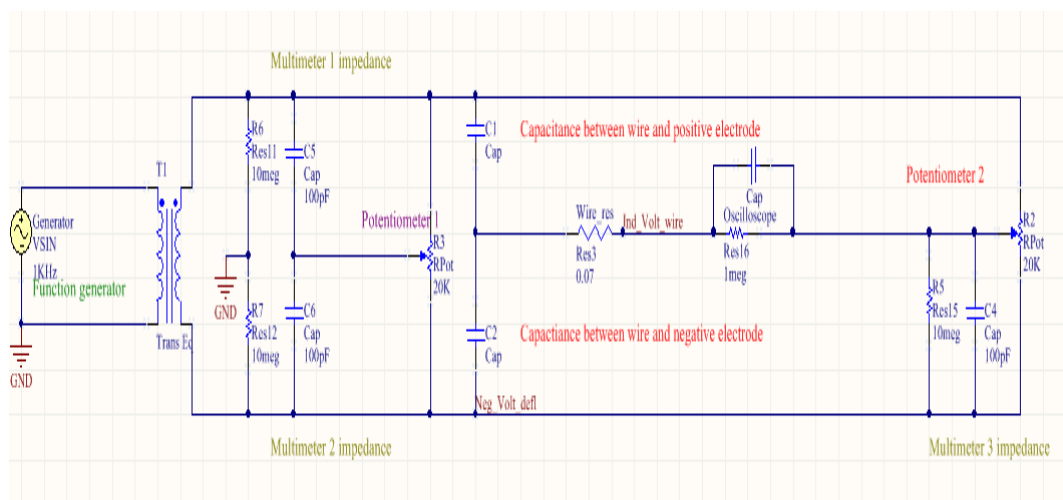


Figure 17— Simulation Model

The model starts with a function generator on the extreme left; the function generator generates 4 kHz sinusoidal waveform with 20 Volts peak to peak. The output of the generator is given to a transformer with 1:1 turn ratio. The parallel combination of R6 and C5 corresponds to the input impedance of a nominal handheld Fluke 175 digital multi meter (accuracy ± 0.01 mA). Similar combinations of R7 || C6 corresponds to multi meter 2 and R5 || C4 corresponds to multi meter 3.

To divide the output of the transformer into 2 symmetric equal voltages, a potentiometer 1 (20 k Ω \pm 20%) is used whose knob is grounded and set at the middle point of it.

The multi meter 1 & 2 monitor the voltage applied to the electrodes. So, that the variation of applied voltage on the electrodes during the measurements is observed.

Finally, following the paper [1] , a high impedance scope is modelled with an input impedance of 1 Meg||14 pF labelled as Oscilloscope, which is the input impedance of Fluke 190 floating oscilloscope. The reason for using this floating scope is that in the normal oscilloscope, common channel is grounded and connected to the source ground as well, while here in order to make precise measurements of the flow of charge from the wire to the potentiometer P2 (used for biasing the wire), it is necessary that there is no leakage of current to the ground.

C1 and C2 are parameterized by using the capacitance measurement data and using the curve fitting model with a quadratic fit equations 15 and 16.

The voltage induced on the wire by sweeping through the position of the potentiometer P2 from 200 Ω to 18 k Ω is shown in the graph below.

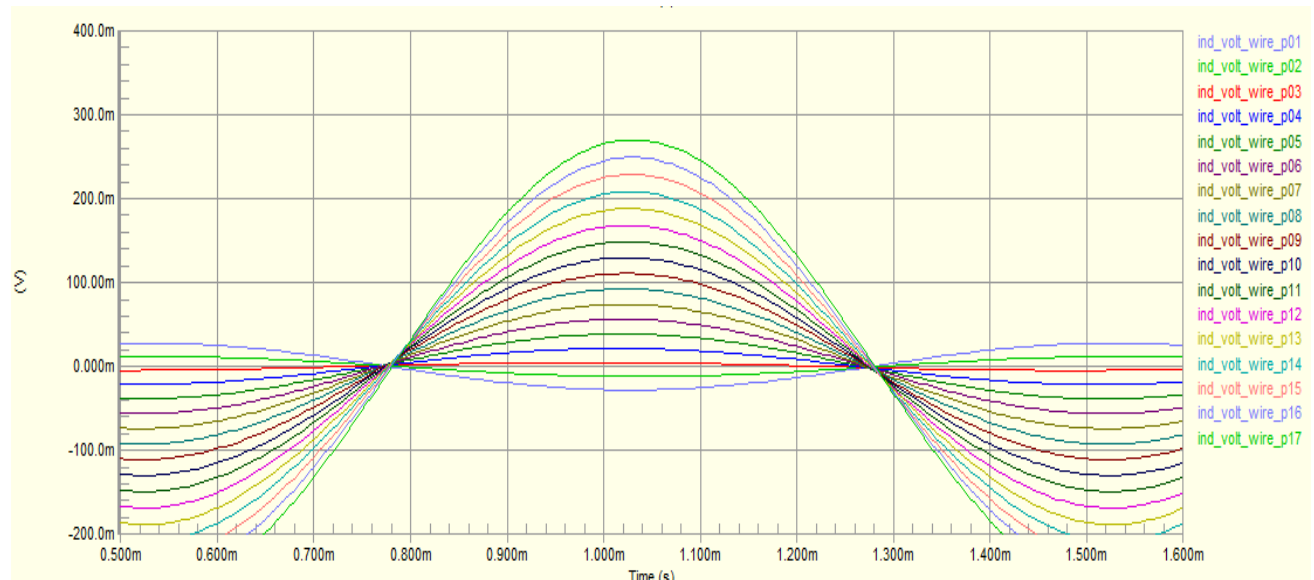


Figure 18. Induced voltage on wire

Since the measured signal appeared to be very small so the impedance of the scope is increased by 10 times and the effect can be seen in the graph below:

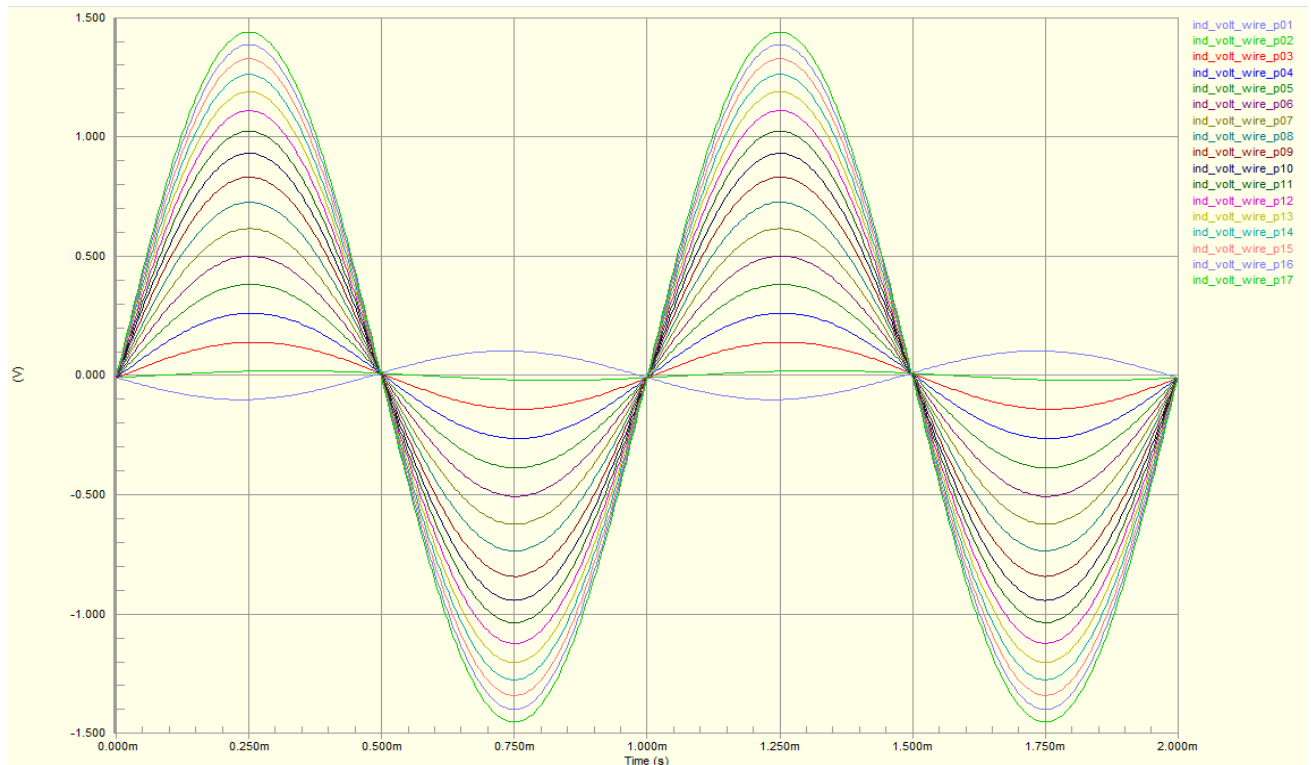


Figure 19. Induced voltage on wire

Moreover, if we decrease this current measurement scope impedance, a phase shift occurs in the signal being produced which is shown in the figure below:

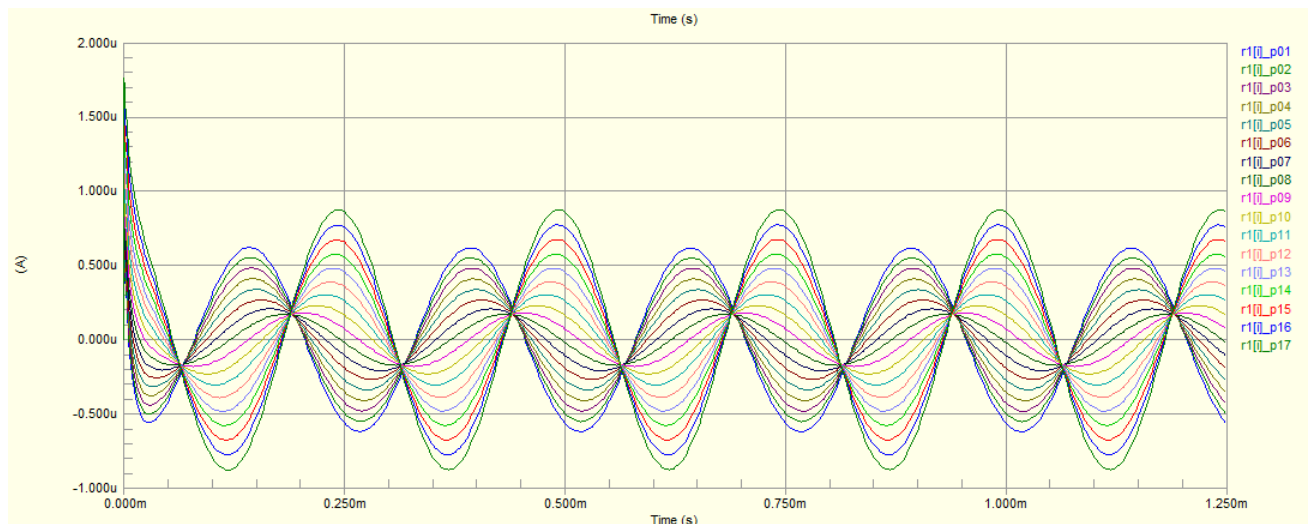


Figure 20. Phase shift of wire signal

From figure 20, if the impedance is lower than 10 MΩ then a phase shifted current signal occurs which is also no longer going to zero as the potentiometer is swept by keeping the

wire fixed at center position ($C1 \approx C2$). Therefore, a high impedance scope of impedance at least $\geq 10 \text{ M}\Omega$ is required. Also, the setup proves that the approach of making the induced voltage go to zero has an outcome which was expected when the wire had been at the right position.

4.1.2 Second Approach

In the previous approach, a problem regarding the very high impedance of the scope values is mentioned, this can be achieved by using an instrumental amplifier connected between the wire and the potentiometer and used as differential amplifier with gain of one.

For a simulation model, the instrumentation amplifier used is INA118 by Texas Instruments. It has input impedance for differential mode up to $10000 \text{ M}\Omega$. Moreover, at gain 1 its bandwidth is up to 800 kHz . Another important characteristic is the input biased current which is limited to 5 nA and the introduction of noise due to the amplifier varies in proportion to the square root of the frequency of operation.

There was no spice model available for the respective instrumentation amplifier, therefore by using the datasheet and respective parameters it is constructed manually and named as INA118. Because of this, the behavior of the amplifier is assumed to differ from the original one but as an initial test for its usage, it can be taken care of later.

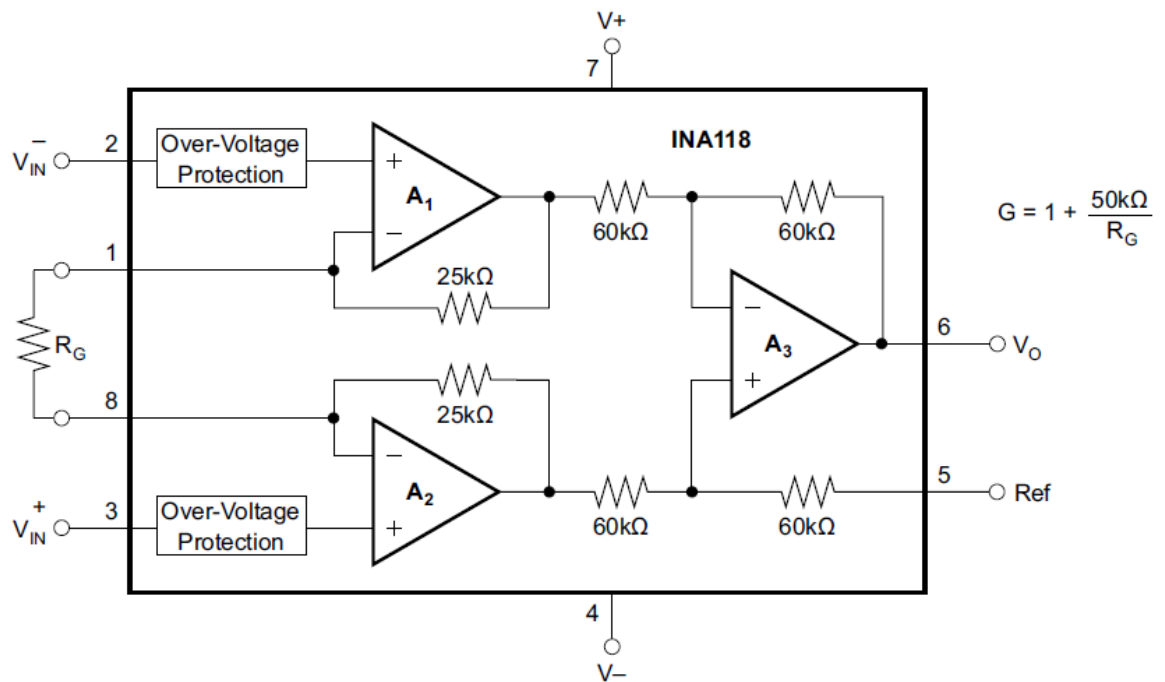


Figure 21. INA118 internal configuration [8]

In figure 20, the same circuit as mentioned in the first approach is used except that insertion of 2 amplifiers. First one is used to measure the difference of the two signals, the voltage from the induced charges and the voltage applied using a potentiometer. Second one is used to nullify the DC offset which may have appeared due to the amplifier 1. But the approach seemed to be very restricted because it can only be used to measure signals of low voltages (not more than 10 V).

For lower voltages, it worked very well. The following graph shows the input signals generated at the two inputs of amplifier. One input is fixed while the other one is swept by changing the potentiometer 2 from 500Ω to 4.8 kΩ.

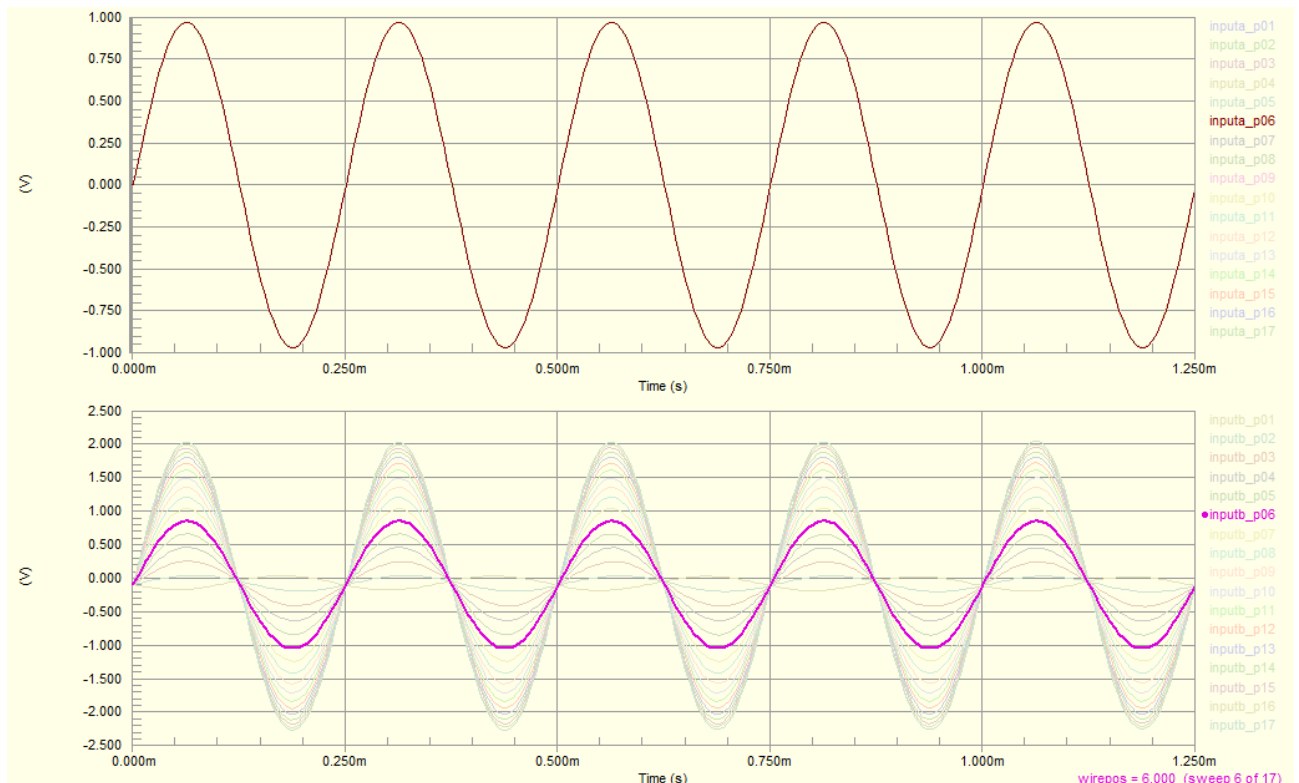


Figure 21. Input voltages to INA118

Also, here, the problem of phase shift of the signal due to the change in position of the potentiometer position (hence the voltage) is also removed.

4.1.3 Third Approach

The third approach employed solved the problem of measurement by using a shunt resistor of very high impedance 1-100 MΩ and measuring the voltage across it. Since the current which is simulated to flow through the shunt can vary from nanoamperes to micro amperes, the measurement signal is prone to noise due to the surrounding 50Hz noise levels. Therefore, to improve the signal to noise ratio, the applied voltage can be increased, additional noise producing components can be removed or replaced and the measurement can be carried out in anechoic chambers (which don't allow the external frequencies or atmospheric frequencies to affect the measurement).

Moreover, a second source is used as a controlled source to avoid the use of motorized potentiometer.

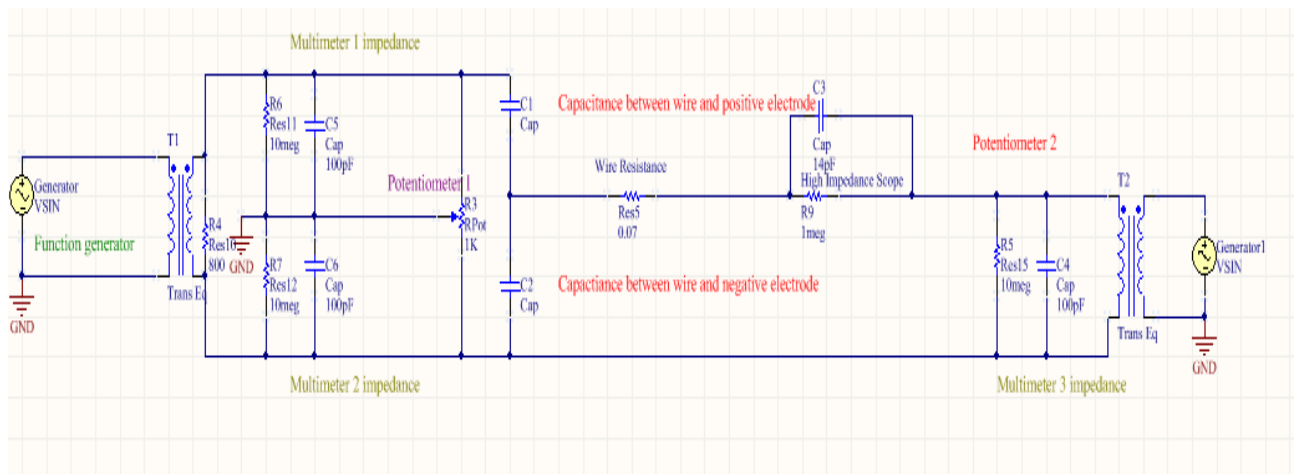


Figure 23.

Since the original circuit contains a potentiometer and to control the voltage, the central knob of the potentiometer should be moved. Therefore, a motorized setup for the movement of the knob is required. The use of two sources for sinusoidal voltage, first one to ensure the symmetric voltage on the plates and second one to give potential to the wire replaces the potentiometer.

The circuit can be used in two ways, one by using negative electrode potential as a reference and the other way is to use the positive electrode potential by connecting the respecting terminals of transformer between wire and the positive/negative electrode terminals. Both connections yield same results.

CHAPTER 5

Electric Field Simulations

5.1 Physics Involved

Before moving on to the final circuit design, it is proposed to verify the field which is about to be measured and to understand the physics of the geometry of the deflector. It can also help in determining the effect of the deflector geometrical design on the field homogeneity and can interpret that how does the variation of geometrical parameters like alignment of the deflector plates can shift the origin point (where field is intrinsically homogeneous up to the required standard factor of 0.001 from the reference).

For this purpose, physics based simulation is done using COMSOL Multiphysics. It is a tool which is based on finite element simulation method. It uses Maxwell equations to solve the model.

$$\nabla \cdot \mathbf{E} = \frac{\rho}{\epsilon} \quad (18)$$

$$\nabla \cdot \mathbf{B} = 0 \quad (19)$$

$$\nabla \times \mathbf{E} = -\frac{\partial \mathbf{B}}{\partial t} \quad (20)$$

$$\nabla \times \mathbf{H} = \mathbf{J} + \frac{\epsilon \partial \mathbf{E}}{\partial t} \quad (21)$$

First step is to define whether 2D or 3D model is created. After that the type of simulation model is selected which is in our case for stationary field and steady state analysis. Also with this, its AC/DC model simulation package provides the platform to carry out simulations using electrical interference and do coupling of the physics with the electrical models. The desired geometry is then allotted with a specific material properties which in our case will be Aluminum since the deflector is made up of that material. There are some solver configurations which set the boundary conditions to solve the model, that just involves using air boundary since we like to simulate in a finite environment with atmospheric air as surrounding. Moving on, meshing of the model is done and the idea is to solve the Maxwell equations for each node of the mesh and display the results.

After the above explanation of how the COMSOL works, we can move forward to our required specific simulation of the deflector. The first simulation is done with 2D models.

5.2 Deflector Model

The dimensions of the deflectors are the same as that of the prototype given for testing.

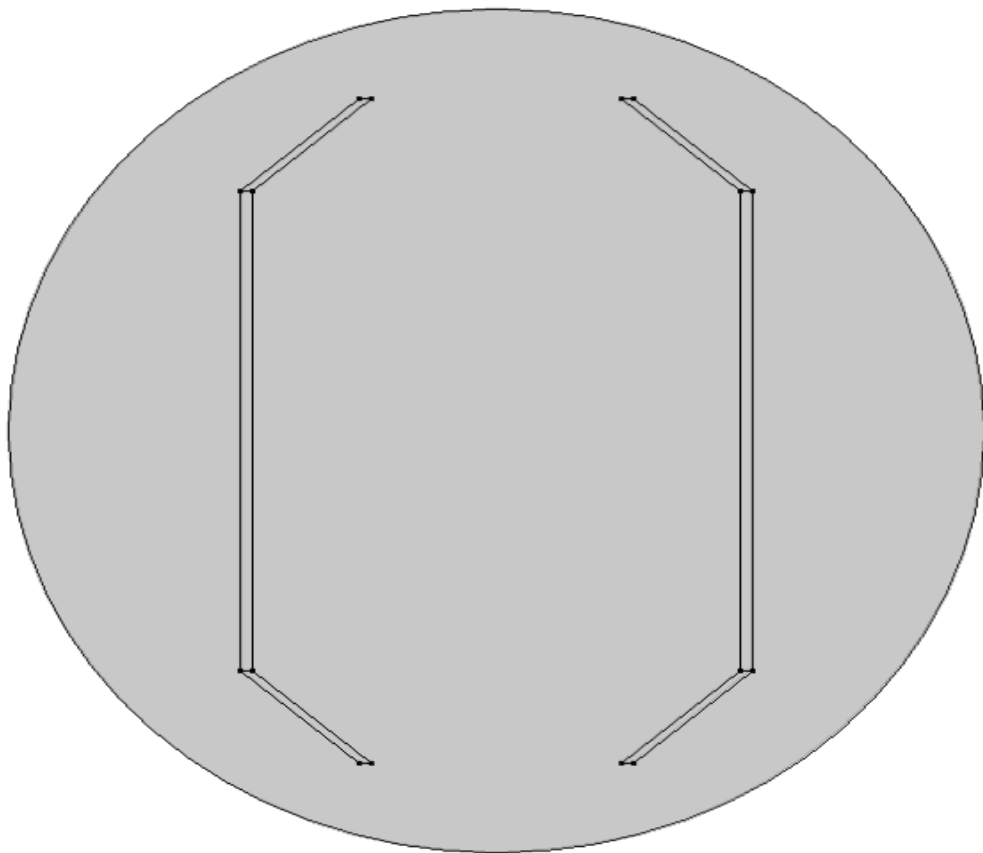


Figure 24.

From the above figure, the plates are not exactly parallel to each other since there are regions where they are bent. This is used to minimize the field fringing at the borders.

A cut plane has been drawn at the center of the plates and equidistant from both vertical ends at the positions from $(-38,0)$ to $(38,0)$, thus neglecting the points close to the deflecting plates because the field is supposed to go to zero on the surface of the plates. A voltage of ± 5 V is applied and the electric field is simulated along the cut line.

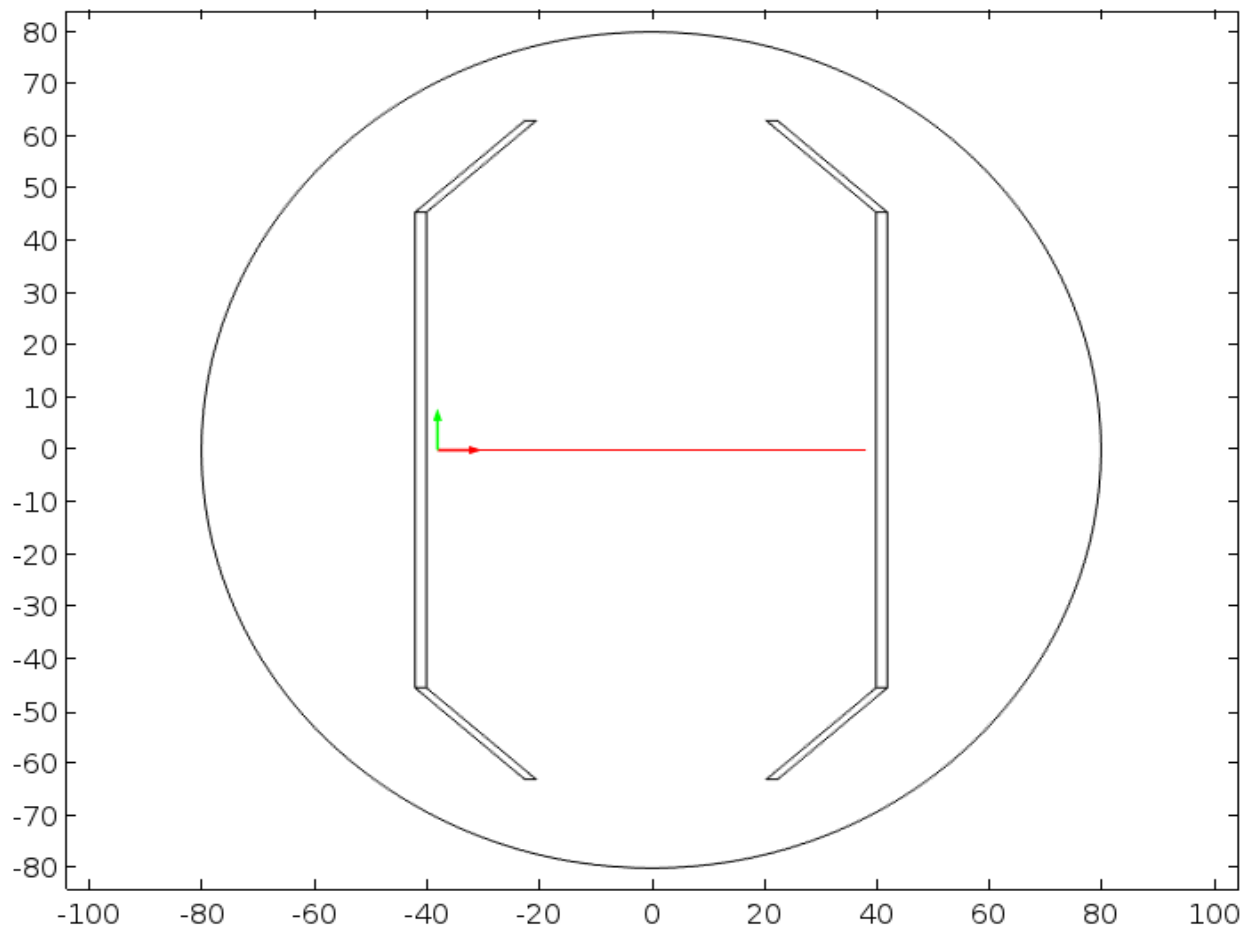


Figure 25. x and y axis are the position coordinates in cm

The electric field is evaluated along this cut line and the resulting plot is observed.

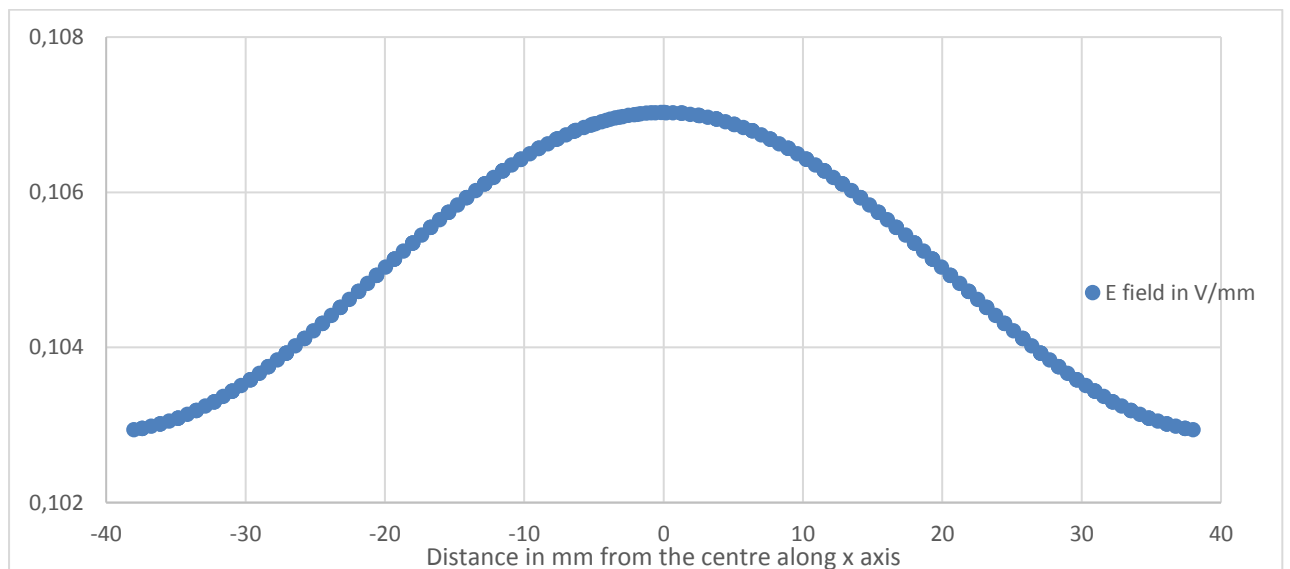


Figure 26.

The above graph is symmetrical which is also in accordance of the theoretical field profile relative to the 'x=0 mm'. This point can be taken as a reference and homogeneity calculations can be done using that value (0.105 V/mm).

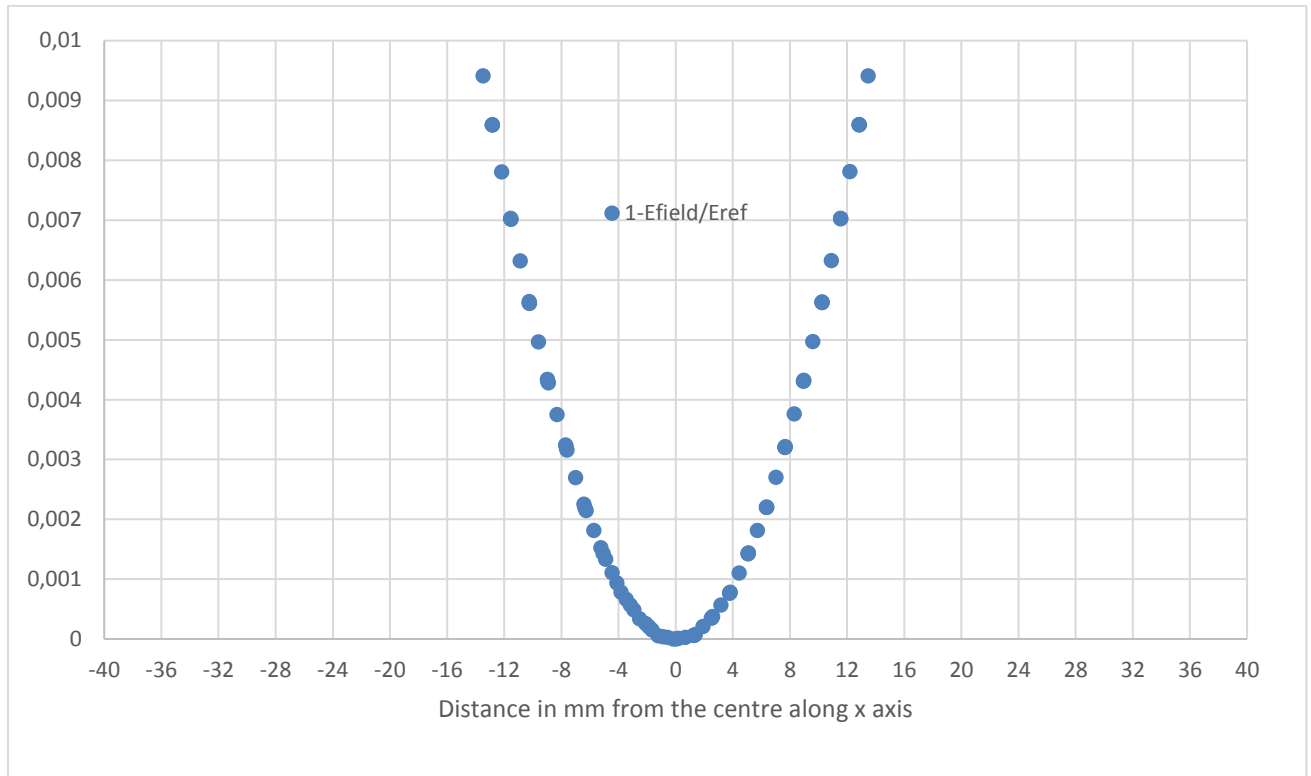


Figure 27.

Graph in figure 27. is plotted using the expression $Y = 1 - \frac{E_{field}}{E_{ref}}$ for every fixed position where E_{ref} is the E field value at 0 mm coordinate. Further following information is deduced from the simulation results that with the medium between the two plates as air and the body of the deflector is grounded, the region of homogeneity lies between -4 to +4 mm from the center with the variation factor of up to 0.001.

Next step is to compare the effect with two parallel plates, another simulation with 2 parallel plates is carried out. The reason is to understand how this geometry can affect the field homogeneity and by how much percentage the region is affected by the position and geometry of the plates.

5.3 Parallel Plates Model

The two curved ends at the top and bottom of the deflector plates are ignored in this simulation.

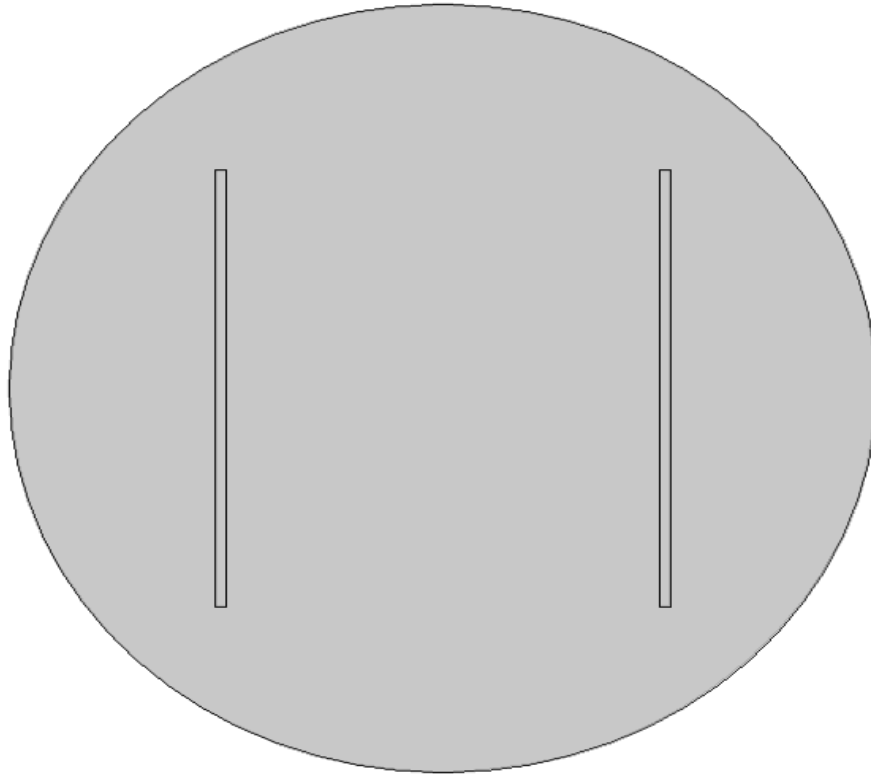


Figure 28.

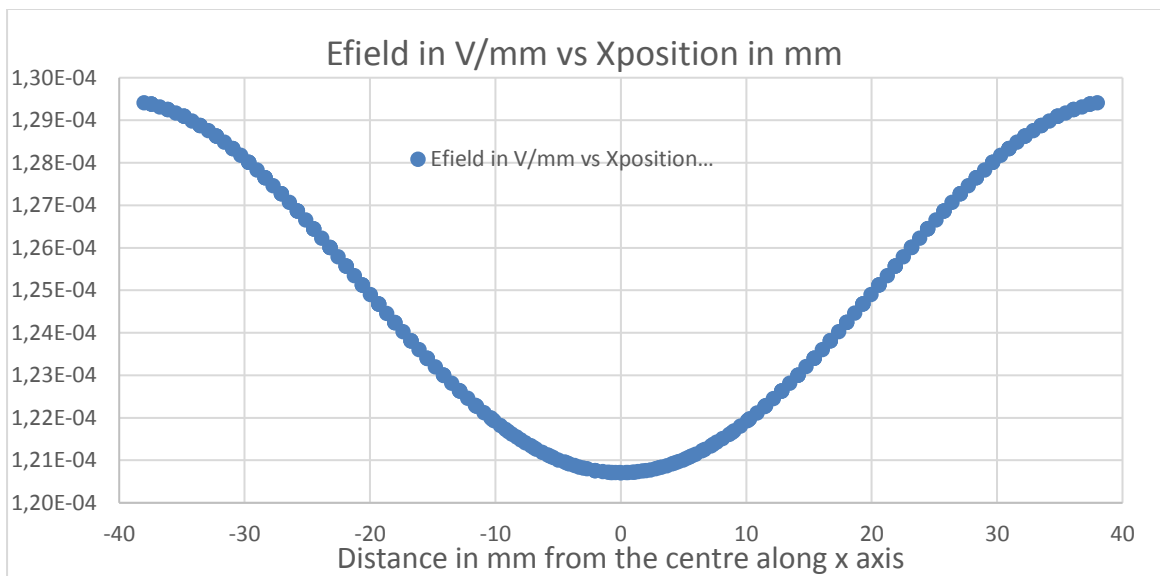


Figure 29.

If we compare the graph in figure 29. with the one in figure 27., they are not the same. The removal of curved ends has affected the profile shape of the E field by making it inverted as was seen before. Now using the same principle equation from section 5.2, the field homogeneity is evaluated using the E field value at the center (0 mm).

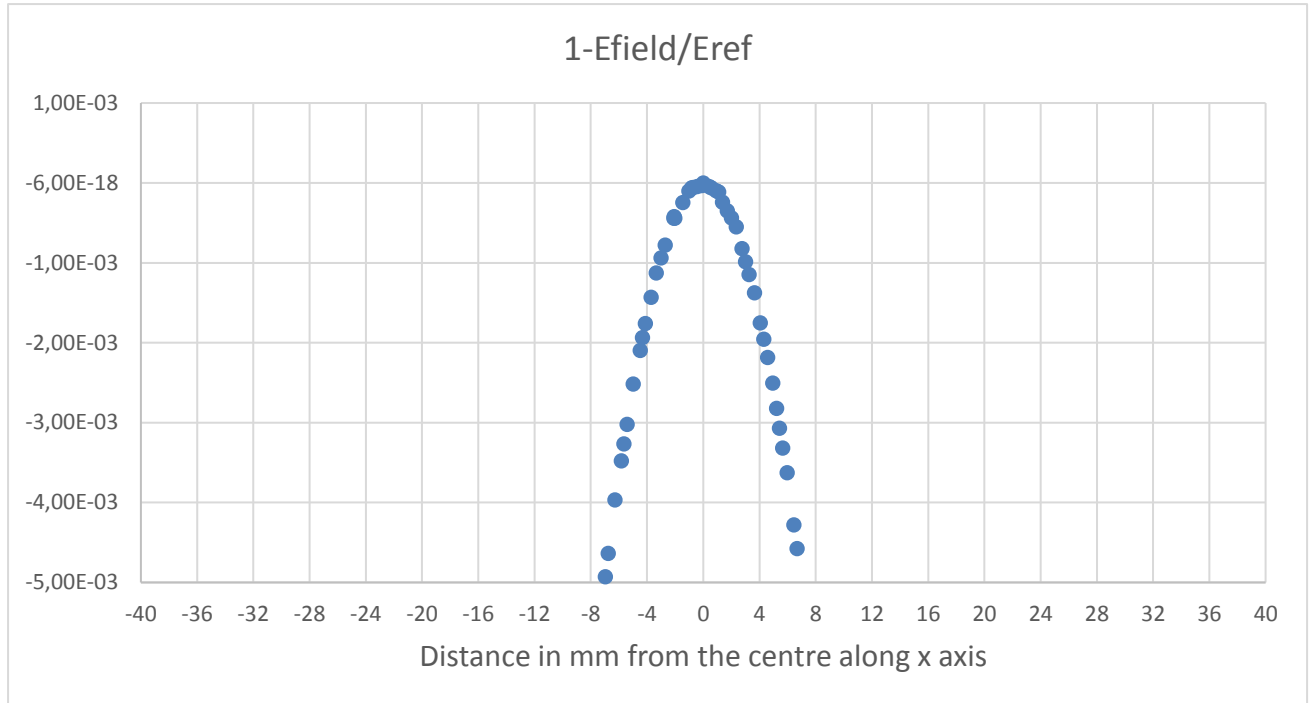


Figure 30.

The region of homogeneity observed from the figure 30. again, lies around – 4mm to 4 mm therefore it shows that the geometry has almost negligible effect on the field homogeneity while it has affected the absolute values and the profile of the field.

5.4 Tilted Plates Model

For an actual deflector installed to bend the beam, the plates are not supposed to be completely aligned and they are designed by tilting one plate with respect to the other.

Rest of the dimensions remain the same but a simulation is done to observe the effect of this tilt on the field homogeneity region. In the geometry being simulated, the curved ends have been ignored as an outcome from the previous simulations that it won't affect the homogeneity calculations and just influences the profile shape which is not very relevant.

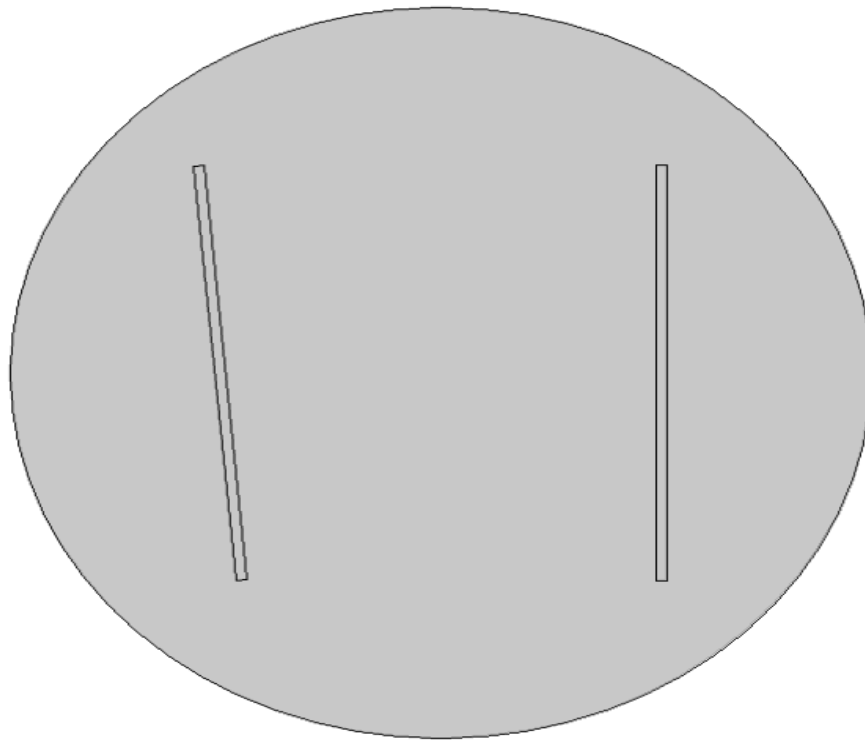


Figure 31.

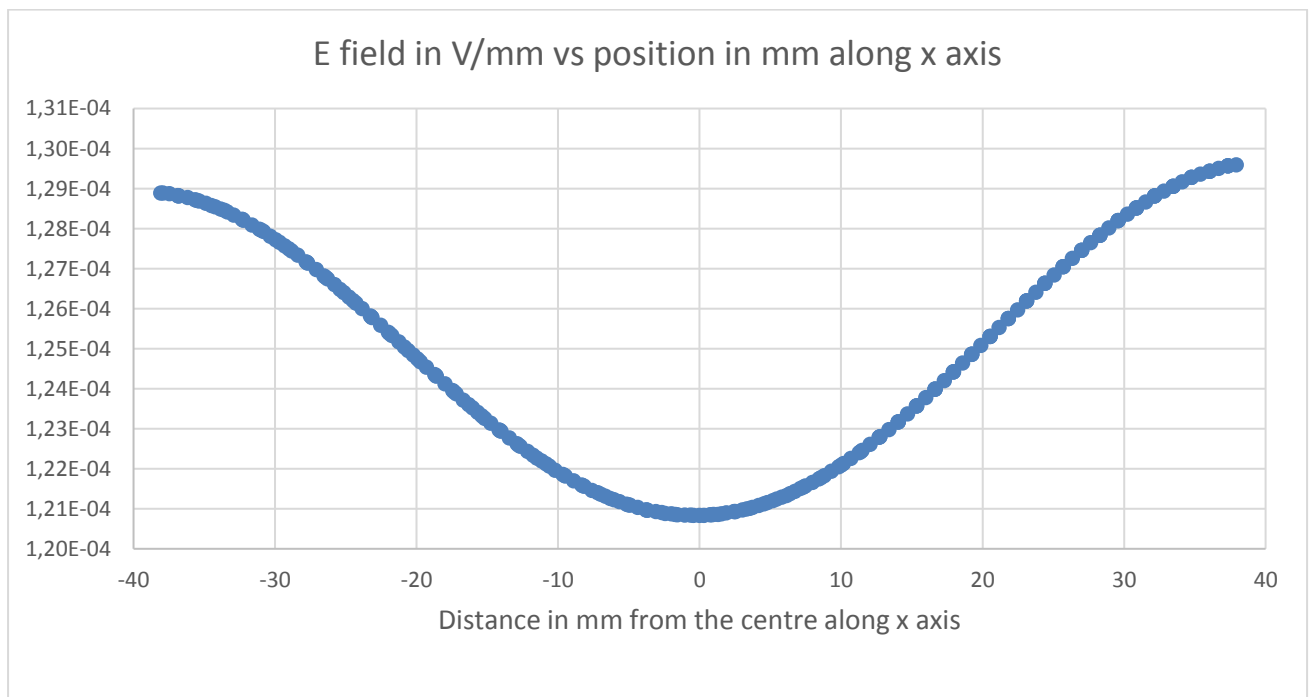


Figure 32.

At first the left plate is tilted by 5 degrees as a reference while maintaining the same potential and other simulation conditions. From the results, as can be seen in the graph of figure 32. that the overall profile shows a shift and more like following the tilt with respect to the parallel plate model simulated before. The region of homogeneity also exhibits a similar shift which can be seen in the graph of the following figure.

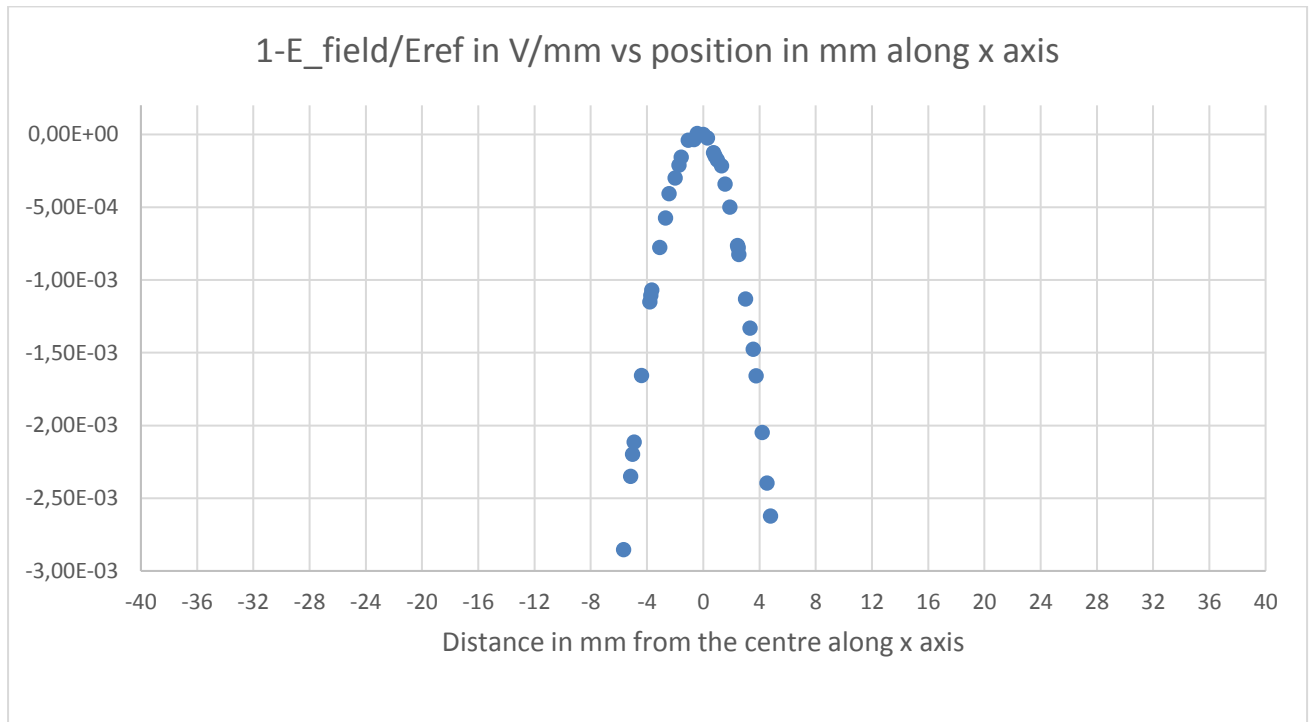


Figure 33.

The values appear to be shifted on the left with more concentration towards the tilted ends. The disturbance in the symmetry is also observed relative to the parallel plates simulation model. But overall the region of homogeneity remains almost around the same location.

If the same operation is performed on the negative plate by tilting it 5 degrees with respect to the positive plate, a mirror effect will be observed as well. For its validity, again one more simulation model is created and results matched with the expectations of very negligible effect on the region of homogeneity.

Because of these simulations, one can infer that after the measurement setup will produce the results, they can be validated by taking these model simulations results.

For the conformity, the last simulation model graphs are also shown below:

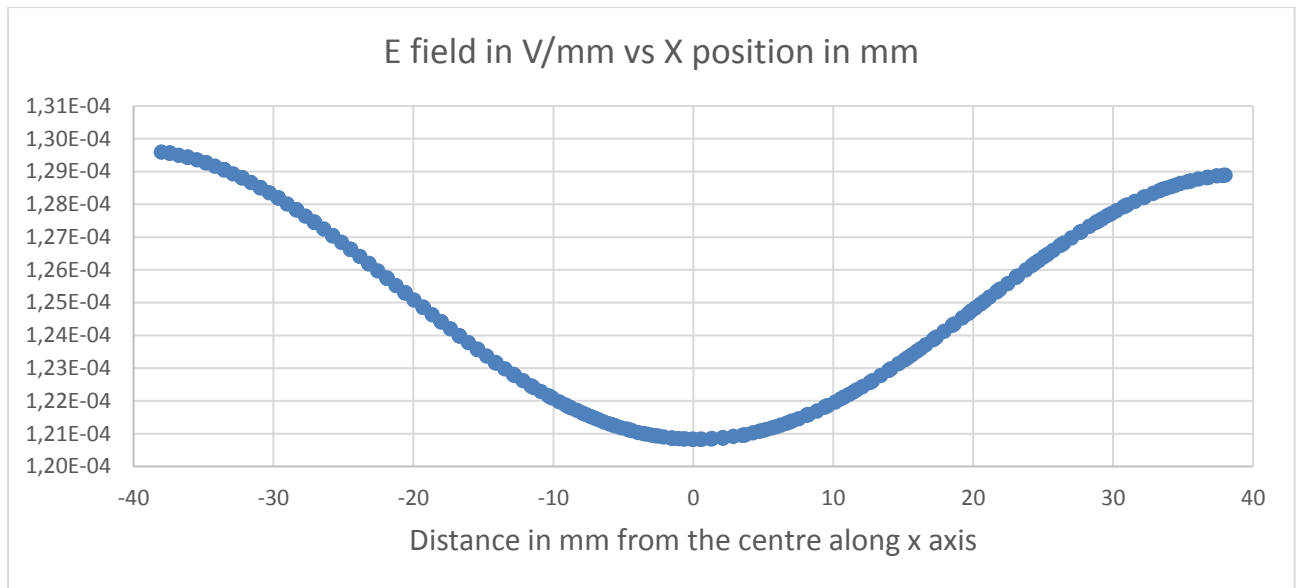


Figure 34.

Also, similarly the homogeneity calculations are done accordingly.

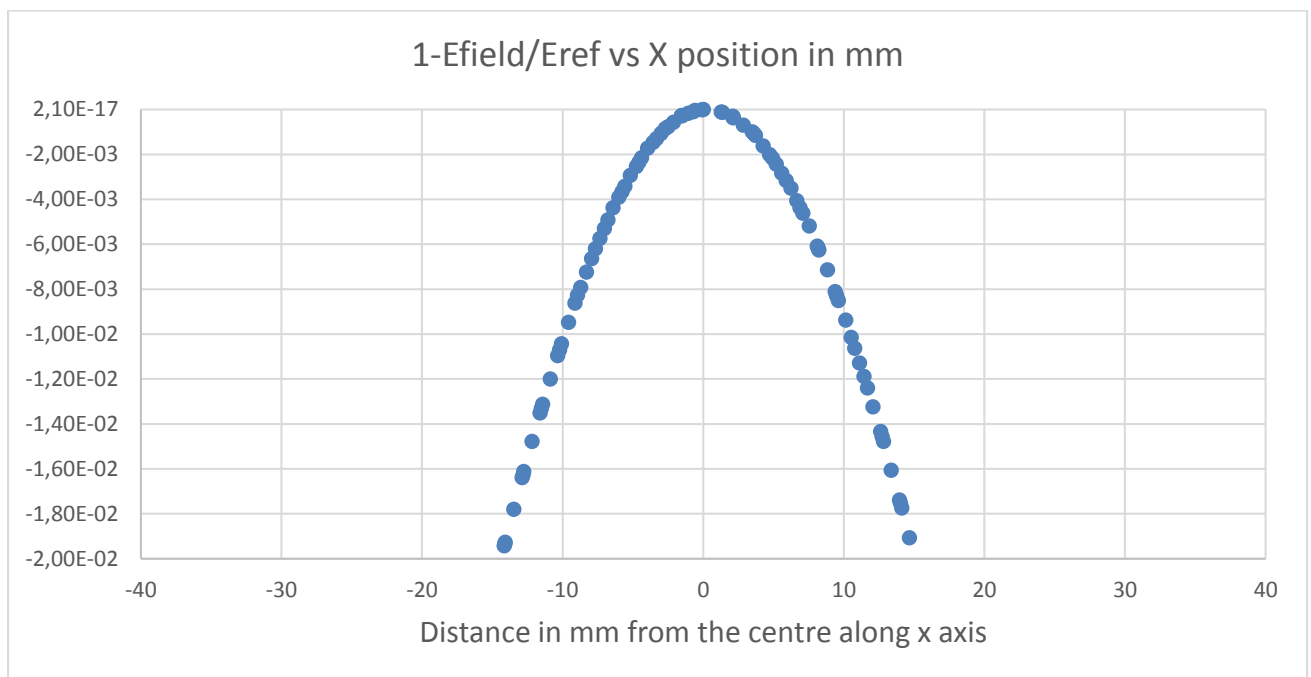


Figure 35.

All the above results indicate that with the method proposed , there exist a region where the required tolerance of field variation can be met.

CHAPTER 6

Hardware selection

6.1 Measurement electronics

The hardware required to build the test bench is divided into two parts:

- 1) Hardware for Acquisition
- 2) Hardware for Wire motion

Hardware for Acquisition:

At the start, a PXI crate has been used with the following specifications:

- PXIe 1071 crate
- PXIe 8100 CPU
- PXIe 4081 High Precision Digital Multi Meter
- PXIe 5402 Analog Output card

6.1.1 PXIe 1071 crate

NI Lab View 2015 is used to program the PXIe system. The PXIe 1071 operates at 220 VAC. Its architecture allows 1 CPU and 3 peripheral cards to be mounted and operated.

The setup being built with this crate is used as an initial setup and therefore is used only for lab measurements. Moreover, PXIe 1071 has a built-in clock which can sample as high as up to 100 Mega samples per second. The architecture of the block also gives an idea about its construction, it is taken from the National Instruments documentation of PXIe 1071.



Figure 36. PXIe 1071 [9]

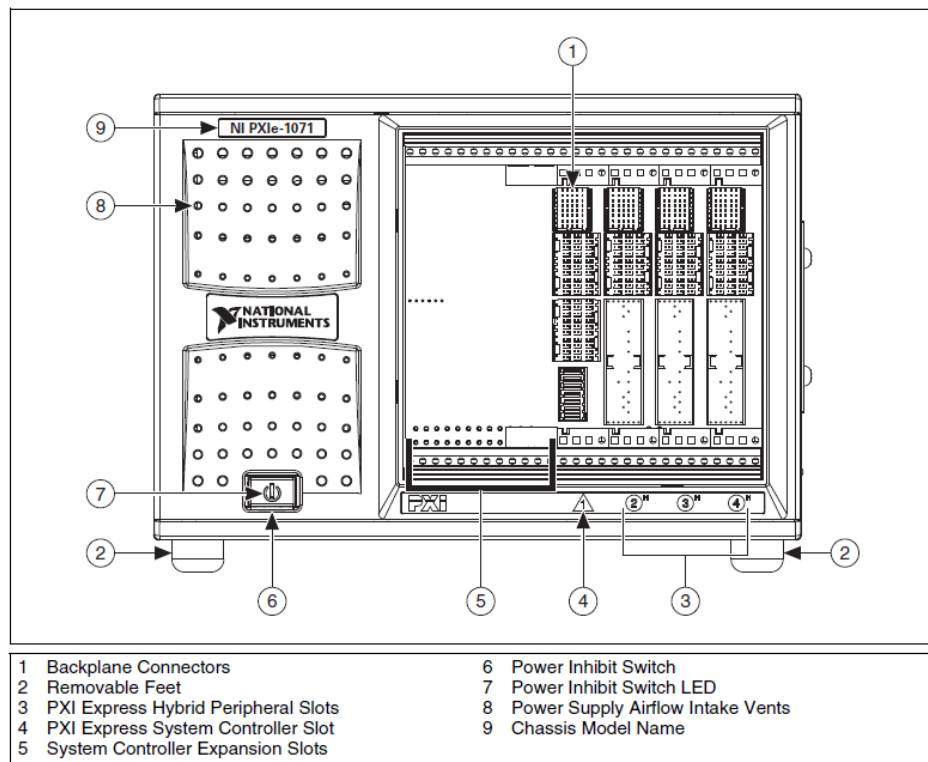


Figure 37. [9]

6.1.2 PXIe 8100

The NI PXIe-8100 is made of using an Intel Atom Processor D410, single channel DDR2 and 667 MHz memory controller. It contains an ethernet slot which can be used to communicate with the device remotely.

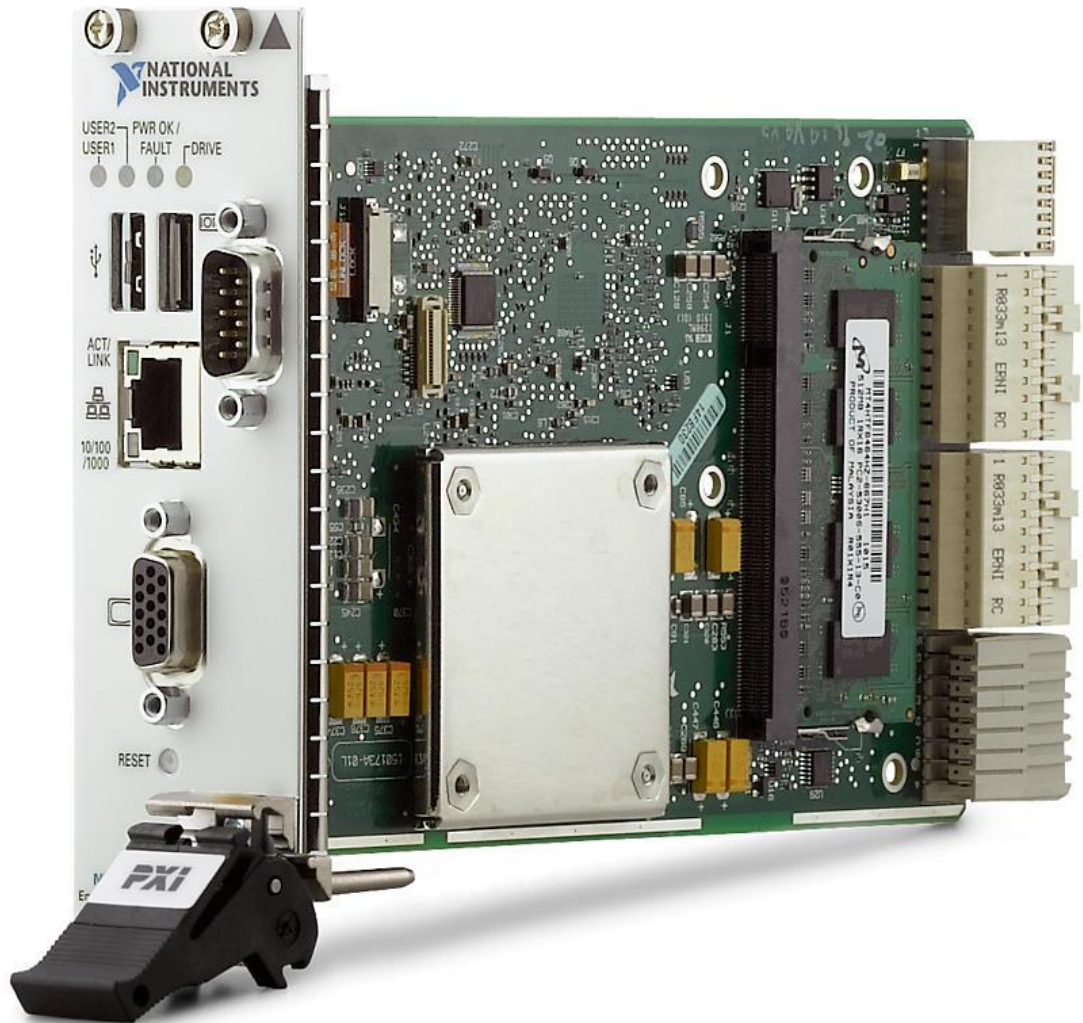


Figure 38. PXIe 8100 [10]

Moreover, the architecture diagram shows that it can be connected to a VGA and resulting waveforms can be displayed as well. Although we are not going to use all the features of PXIe 8100 but it just provides an overview of the architecture, following diagram can be used for further explanation as taken from the reference manual of NI- PXIe 8100 user manual. Moreover, the specifications information is also taken from the user manual of the NI-PXIe8100.

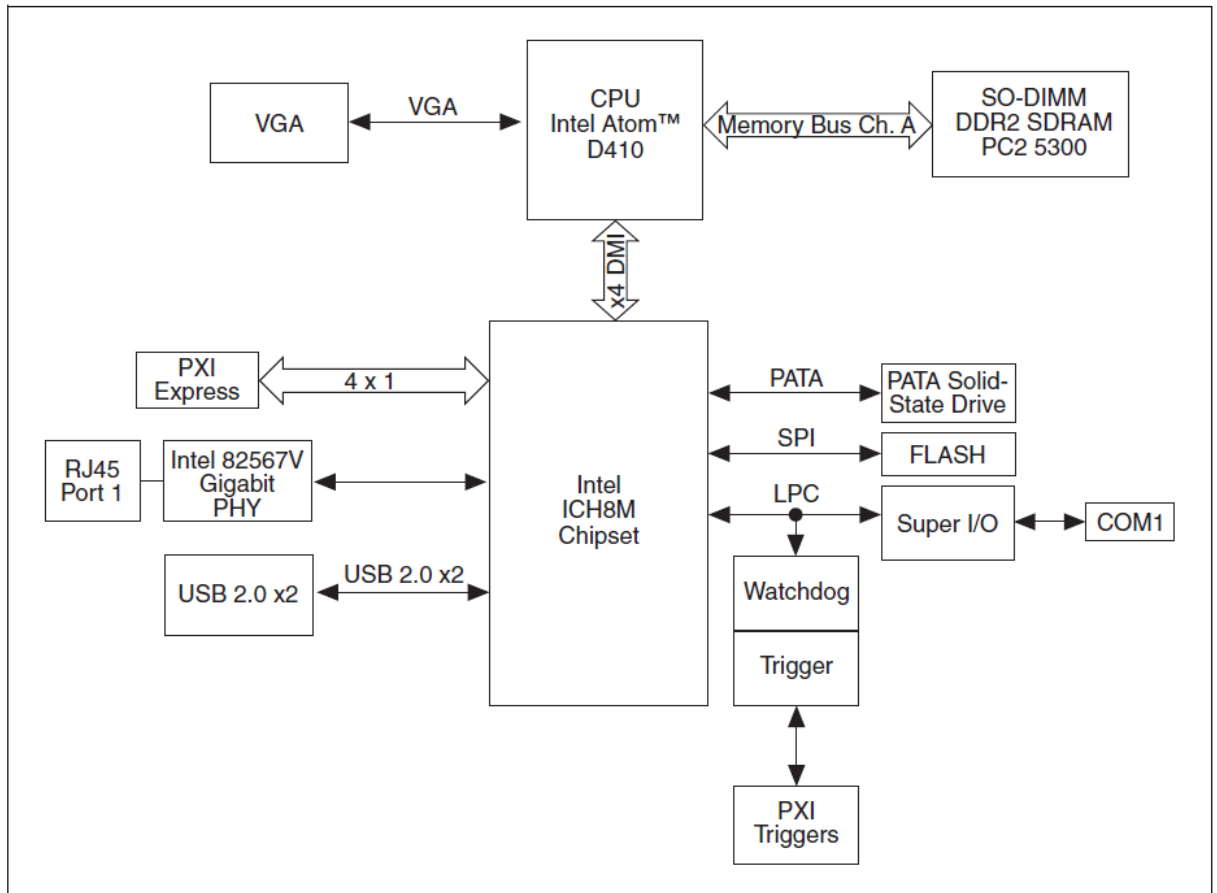


Figure 39. PXIe 8100 architecture [10]

The logic blocks shown in the figure above are the following:

- Intel Atom processor D410. [10]
- The *SO-DIMM* block consists of one 64-bit DDR2 SDRAM sockets that can hold up to 1 GB. The *CPU* connects to the DDR2 SDRAM, VGA, and Intel ICH8M chipset. [10]
- The *Intel Atom Processor D410* drives the graphics. [10]
- The *Watchdog Timer* block consists of a watchdog timer that can reset the controller or generate a trigger. [10]
- The *Intel ICH8M* chipset connects to the USB, Parallel ATA, PXI Express, and LPC buses. [10]
- The *USB Connectors* connect the Intel ICH8M chipset to the Hi-Speed USB 2.0 interface. [10]
- The *Parallel ATA Solid-State Drive* is a 512 MB storage device. The Parallel ATA interface enables transfer rates up to 17 MB/s in read and 5 MB/s in write. [10]

- The *PXI Express Connector* connects the NI PXIe-8100 to the PXI Express/Compact PCI Express backplane. [10]
- The *Super I/O* block represents the other peripherals supplied by the NI PXIe-8100. The NI PXIe-8100 has one serial port. [10]
- The *Intel 82567V Gigabit Ethernet port* connects to either 10 Mbit, 100 Mbit, or 1,000 Mbit Ethernet interfaces. [10]

6.1.3 PXIe 4081

PXIe 4081 is a 7^{1/2} digit multimeter with a digitizer of 1800 k samples per second.



Figure 40. PXIe 4081 [11]

It can measure 2 different voltage measurements and has channels which are isolated from the ground by a very low capacitance whose value is not provided in the reference manual.

In case of AC voltage measurements, the input impedance of the voltmeter is up to $10\text{ M}\Omega \pm 2\%$ in parallel with 90 pF and the accuracy of the measurement depends on the amplitude of the voltage measured, the range and the frequency of the signal. For our case, we like to perform measurements from 400 to 4 kHz , the accuracy is 0.01% of the measurement + 0.02% of the range. Moreover, the performance of the digitizer also decreases if 2 measurements are simultaneously taken.

In case of AC current measurement, only one measurement is possible. The accuracy for the current measurement depends on the amplitude, peak, burden voltage and the frequency of operation. For the measurements in the range of micro amperes, with peak amplitude of $100\text{ }\mu\text{A}$, frequency of operation of up to 5 kHz and burden voltage of 60 mV we have the accuracy up to 0.065% of reading + 0.02% of the range.

For the measurement of voltage and current, 2 cards of NI 4081 are being used. One for the measurement of current and the other for the measurement of voltage. Following image shows the 2 separate VI for the measurement of current and voltage

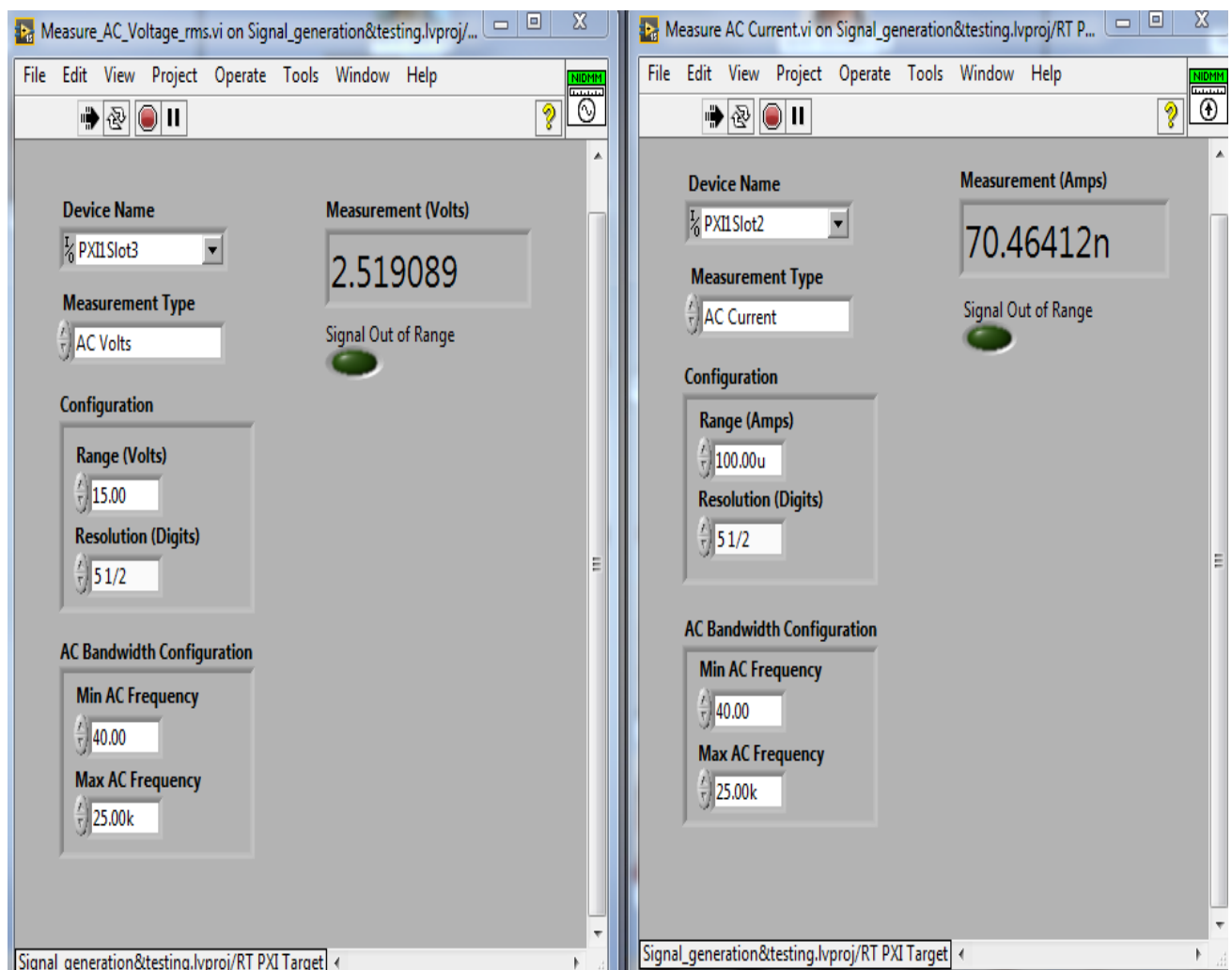


Figure 41.

6.1.4 PXI 5402

PXIe 5402 is an analog output card. It is used to generate the analog output signals which in our case is the voltage waveforms for the deflector inputs. It is a 16-bit device and has the sampling clock of up to 20 MHz

Analog output card has 2 output channels therefore both channels are being used (one for the excitation of the deflector plates and other for the excitation of the wire). The front-end view of the VI used for the generation of these sinusoidal is shown below:

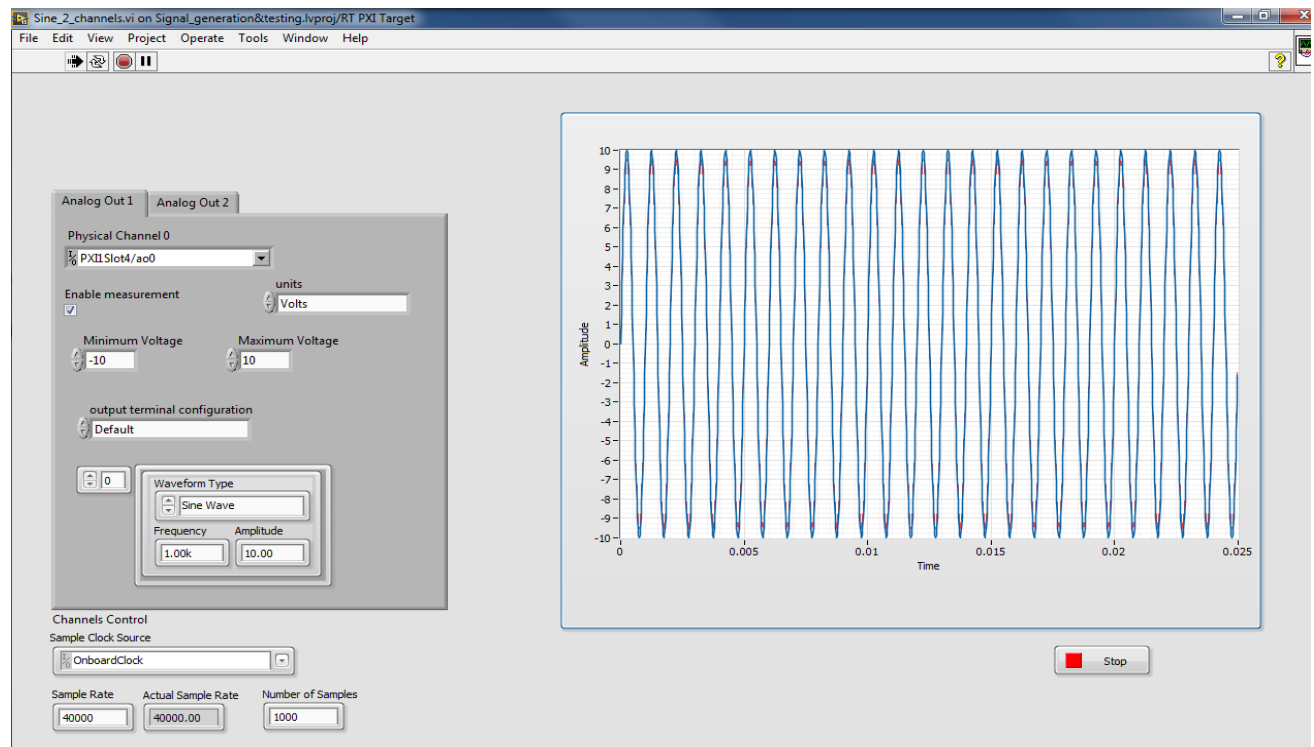


Figure 42.

With the PXIe devices, the tests were performed initially but the hardware required for the motion of the wire was still a question. Therefore, the motion is carried out by hand which produced accurate results and the quest for finalizing the hardware for the motion remained continued.

A collaboration from the magnetic measurements lab helped in using the setup already being used for the magnetic axis measurements for the septum magnets. The next task was to use the existing setup at the magnetic measurement lab and to integrate our existing setup to match with the requirements. Therefore, a complete modelling of the hardware was required which should have contained all the features which had been mentioned above.

CHAPTER 7

Final Design of the test bench

7.1 Remodeling of the circuit used

As mentioned at the end of chapter 6, there was a need of adjustments in the hardware with the existing setup presented at the magnetic measurements laboratory. The updated hardware list included the following instruments as well:

1. 2 audio transformers with 1:1 ratio (E187A)
2. A potentiometer of 8.4 k Ohm (22 turns)
3. A shunt resistor of 20 Ohm
4. 2 Keithley 6221 Current Generator Source

7.1.1 Keithley 6221

Keithley 6221 is chosen as based on the experience from the magnetic measurements lab to use as a current source and shunt impedance can be used to convert it to a voltage source. The key feature of the generator is explained in the following diagram taken from the reference manual of 6221.

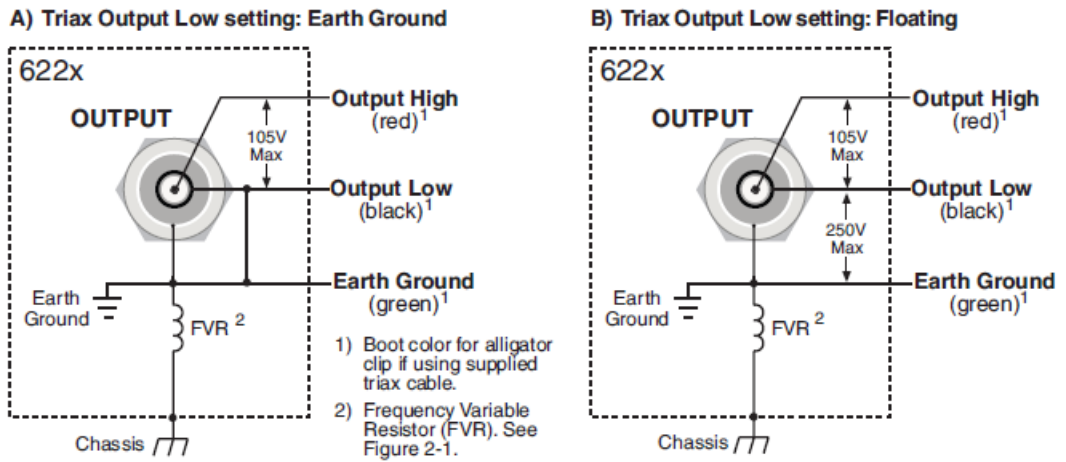


Figure 43. Keithley 6221 output configurations [12]

It gives us the flexibility to generate the current by using floating output terminals settings as well as grounded.

Moreover, it can produce sine wave and arbitrary waveforms using a remote operation. For an automated setup, the remote operation is the key.



Figure 44. [12]

7.2 Grounded measurement model

The final design of the measurement circuit is simulated again using the following simulation model:

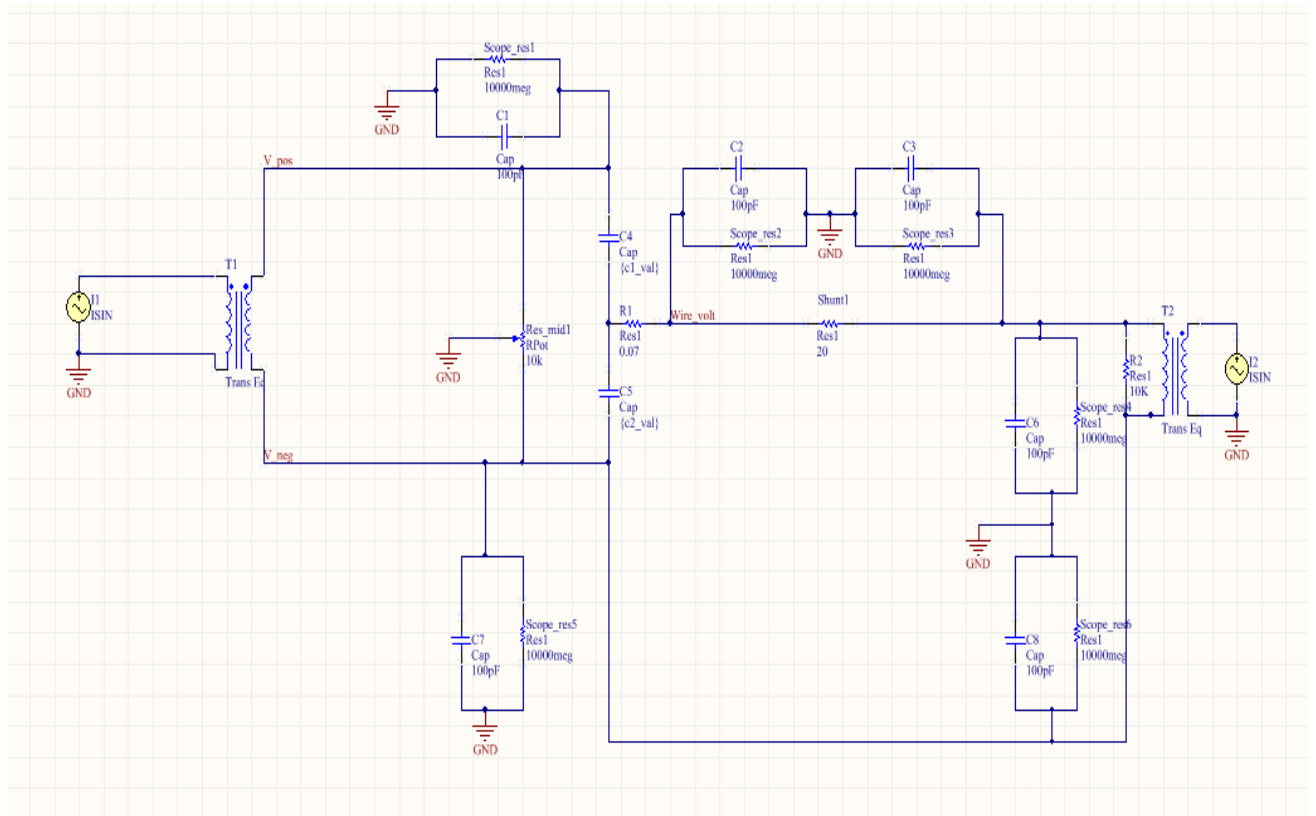


Figure 43.

The circuit is modified by using 2 current sources with shunt resistors to generate a voltage source out of a current source. For source 1, the potentiometer itself can be used as a shunt resistor of value 10 k Ω , so to produce a 10 V output; a current of 1 mA is required to be generated from 6221. The measurement of the voltages is being done with respect to ground. A shunt resistor of 20 Ω is used to measure the current by calculating the voltage drop across it. The second source which is the second transformer provided an isolation with an output resistor at the secondary side converting it to a voltage source. The measurements are taken with respect to the ground and the simulation is done by putting the specific impedances of the voltmeters.

Again, the problem of the signal phase shift appearance is observed which made us to drop the idea of using the voltage across the 20 Ω resistor. Moreover, when the signal is measured using the NI 4081 multimeter, at the time of sampling the signal it got distorted

because the measurement channels were not perfectly isolated from the ground connections.

Therefore, the use of Keithley 2000 multimeter is done. For the final circuit, Keithley 6221 and 2000 multimeter both in twice quantity are deployed.

7.2.1 Keithley 2000

Keithley 2000 is used as a multimeter which is still $6^{1/2}$ but has a higher input impedance for AC voltage measurements. Moreover, the measurement channels are completely isolated for the measurement of voltages.

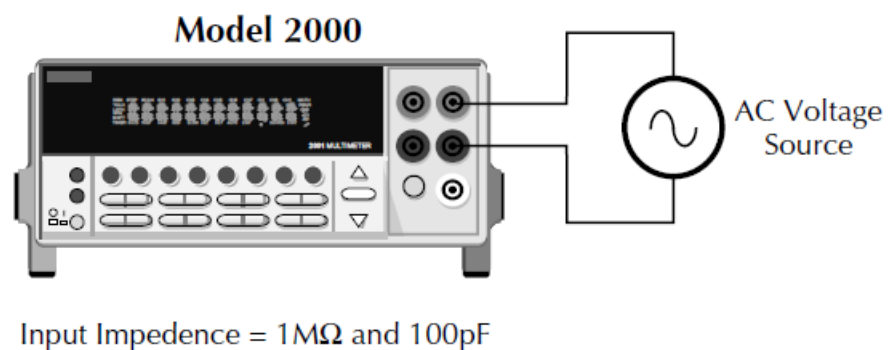


Figure 44. Keithley 2000 [13]

Also, the remote operation using a GPIB bus connection with RS-232 communication port can be used to perform automated operations. The measurement accuracy of the multimeter depends on the range of the measurement, temperature, resolution and range.

For our measurement setup, at 25 degrees Celsius with resolution of $1\mu\text{V}$ of 4 kHz and range in 1-10 V the uncertainty is $\pm (0.05\% \text{ of reading} + 0.03\% \text{ of range})$.

7.3 Final simulation model

Furthermore, the circuit is again modified in such a way to incorporate the changes of using two current sources and 2 Keithley multimeters. One of an important change done is that one end of the wire is ground through the Keithley multimeter and the internal impedance of the voltmeter is used to measure the voltage difference between ground and the induced voltage wire terminal. The idea is again to minimize the flow of current from the wire to the ground.

This change of grounding the wire came from the fact that although floating measurements are the best in such scenarios but there are not 100% floating terminals exist and the

capacitance to the ground will cause some current to flow, therefore the plan is to measure everything with respect to ground and observe the measurements if they make sense or not.

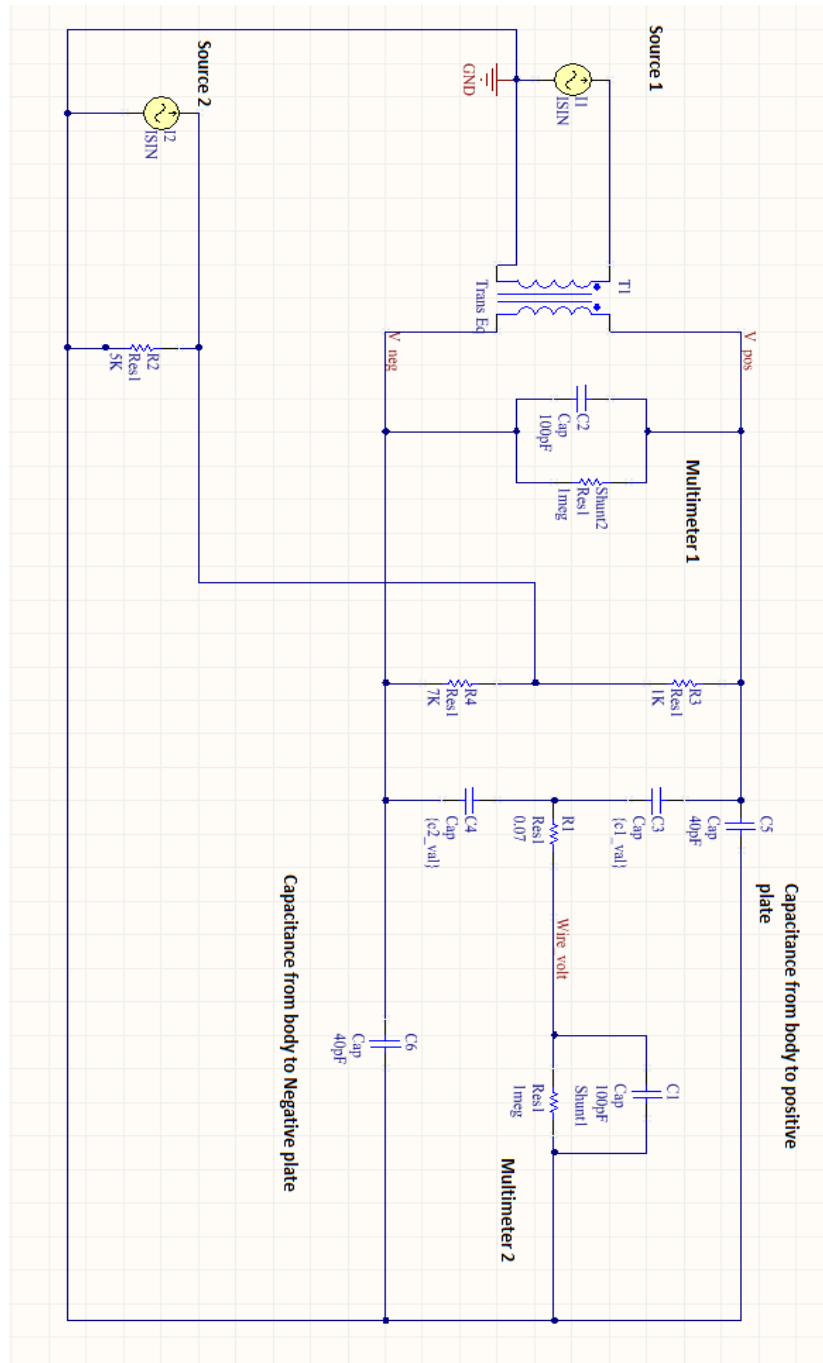


Figure 45.

This method is tried by grounding the wire through a 1 meg Ohm impedance of the multimeter. By changing the symmetry of the voltages on the plates, the origin where the net induced voltage on the wire goes to zero is shifted. Moreover, by using this, we have no strict requirement to use a floating scope or multimeter probes. The new circuit is again simulated to understand and validate its functioning.

In the above figure, Source 1 is used to fix the voltage difference between the plates. Source 2 is varied to make a sweep of change in current. Source 1 is configured to provide 8 mA and source 2 is swept from 500 μ A to 1600 A. Two multimeters M1 and M2 measure the voltage difference across plates and shunt.

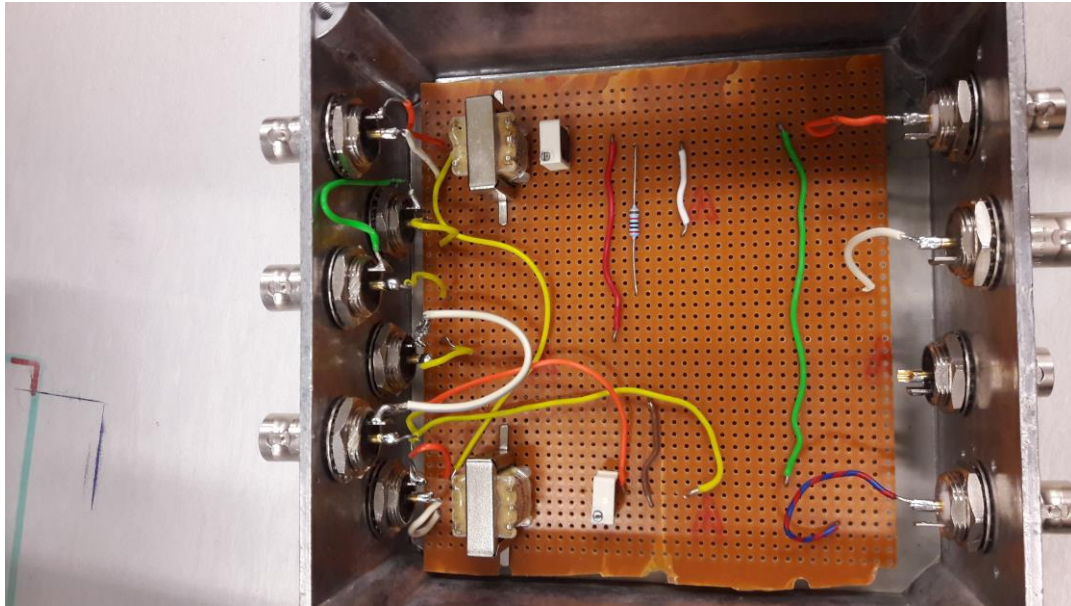


Figure 46. Circuit box

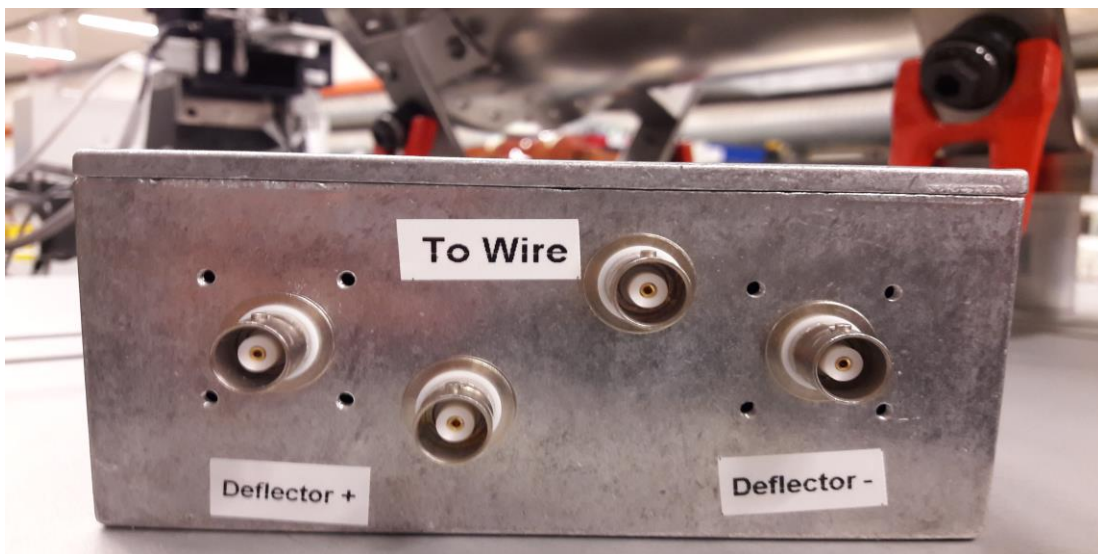


Figure 47. Connections to the deflector and wire



Figure 48. Connections for the excitations and measurement signals



Figure 49.

7.4 Synchronization of the generators

The 2 Keithley 6221 current generators were not synchronized and they had to be synchronized to start the measurement. Moreover, the 2 sources were not sharing the same clock and there was a difference of 1 mHz between the 2 for a frequency generation of 4 kHz. This relation of frequency difference was not linear with respect to the amplitude of the signal.

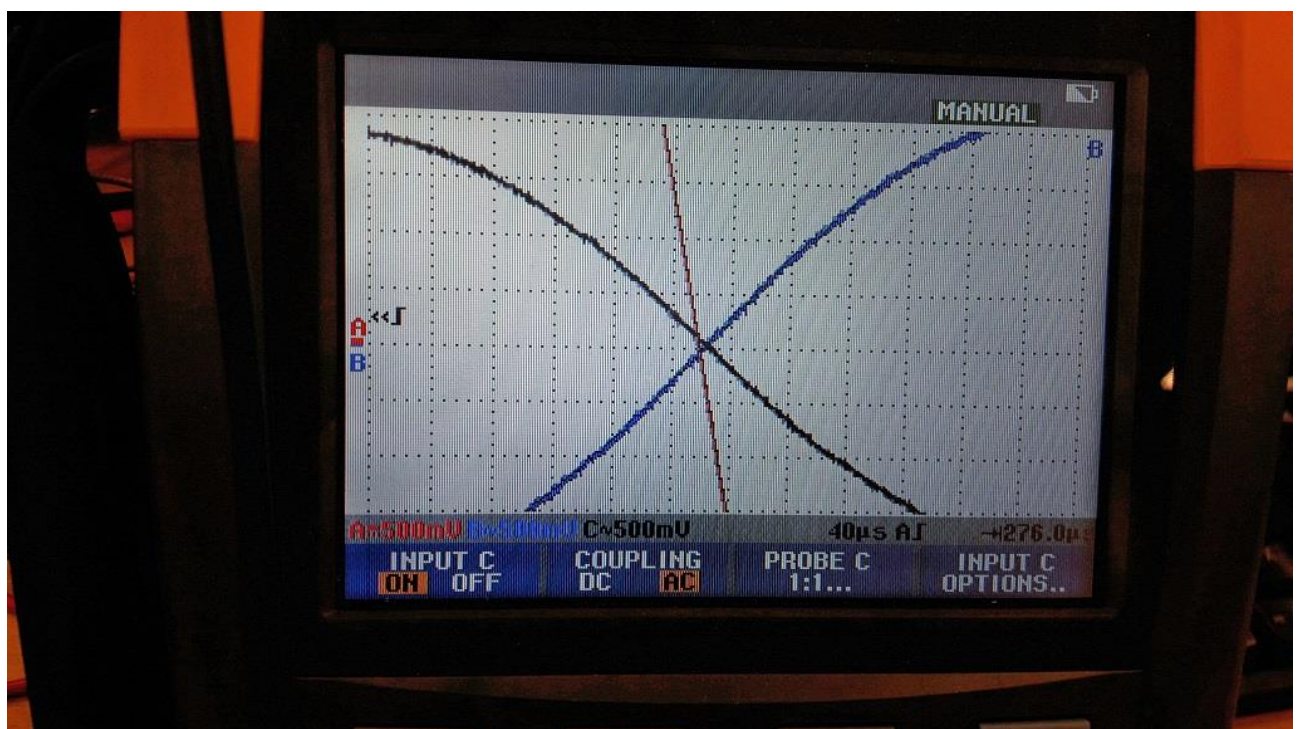


Figure 50.

The delay problem has been solved by using a trigger option provided in Keithley Generator. A cable is connected from one generator to the other one and Source 1 is configured to send a pulse of 1 μ s with the falling edge when it starts generation. Source 2 is configured to start its generation on the reception of this falling edge. In this way, the delay problem was solved.

But after careful observation of 2 generated signals, it was observed that one signal is travelling faster as compared to other. Hence there was a frequency difference between the 2.

It was not possible to solve this issue with this setup; therefore, both the sources were configured in such a way that during the sweep, both start, stop, reset and start again for

every measurement. Hence, they start at the same time and the acquisition is done right after that.

The problem is solved by triggering both the sources together from the controller. Thus, resulting in an approximately synchronous measurement. Moreover, an additional delay of 1 ms was added between a start and reset by keeping in mind the sampling rate of 100 k samples per second of the acquisition card so that a stable value of the measurement is done.

7.5 Hardware for the wire movement

For accurate position measurements and control, PI motors are used. In total 5 motors are used. One for controlling the tension of the wire. While 4 motors, 2 for x-axis movement of both end of the wire while 2 for the y-axis movement of the wire are used.

The stages for the motion can move and measure the position up to 1 μm resolution. For our setup, the precision required was 1 mm and with the use of PI precise motion control DC motors, it is easy to use it for out applications.

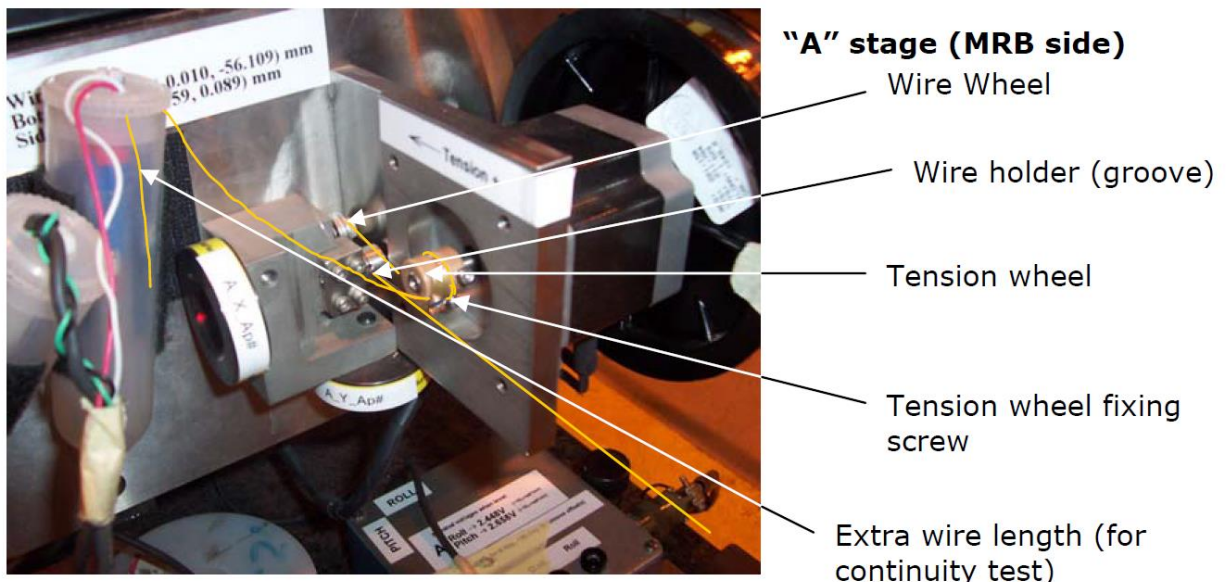


Figure 51. [14]

The wire movement system contains 2 motion stages A and B. each stage contains 2 positioning motors which are used to position the wire. Although the stages can be itself moved along the z-axis plane. These stages were designed initially to test for large size magnets to determine their magnetic axis. The stages are used as it is with their drivers already made available.

The uncertainty in the measurement of the position is $\pm 0.05 \mu\text{m}$.

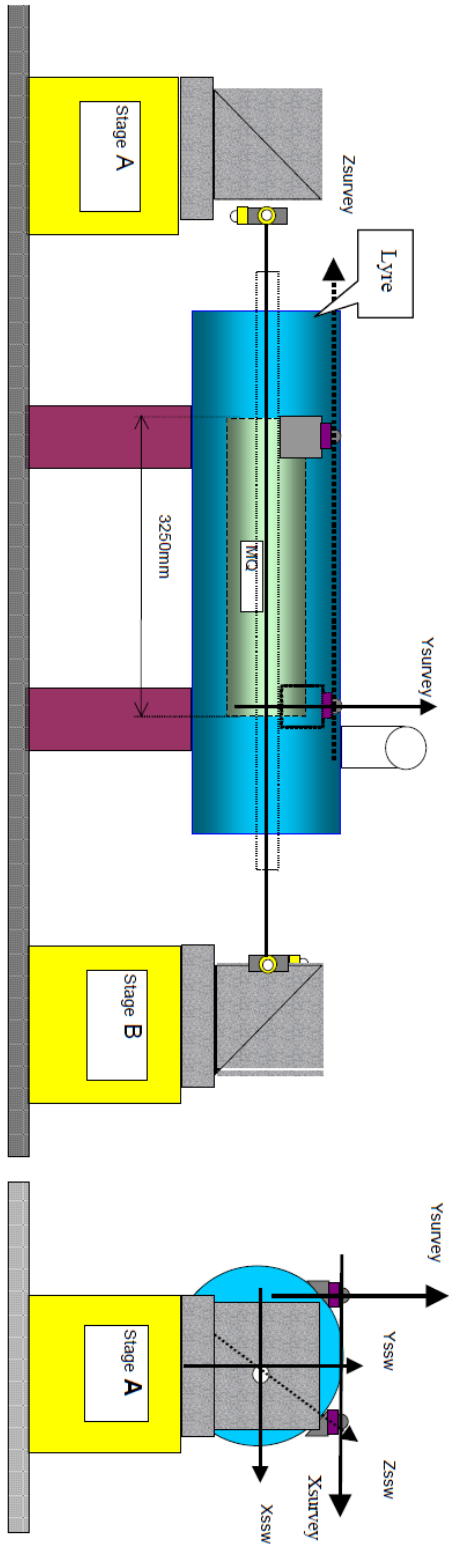


Figure 52. [15]

CHAPTER 8

Implementation and results

8.1 Scripting for drivers

The hardware components chosen can be controlled by writing their drivers for remote operation through C language. Ni equipment's, Keithley and PI motors all can be controlled using a C-script.

C++ language is used to script the first measurement algorithm, which is based on acquiring values at various positions with the set of different voltages applied to the wire. As a result, the data is stored in txt files. A script in MATLAB is imported as a library and is used to carry out the final analysis and make plots.

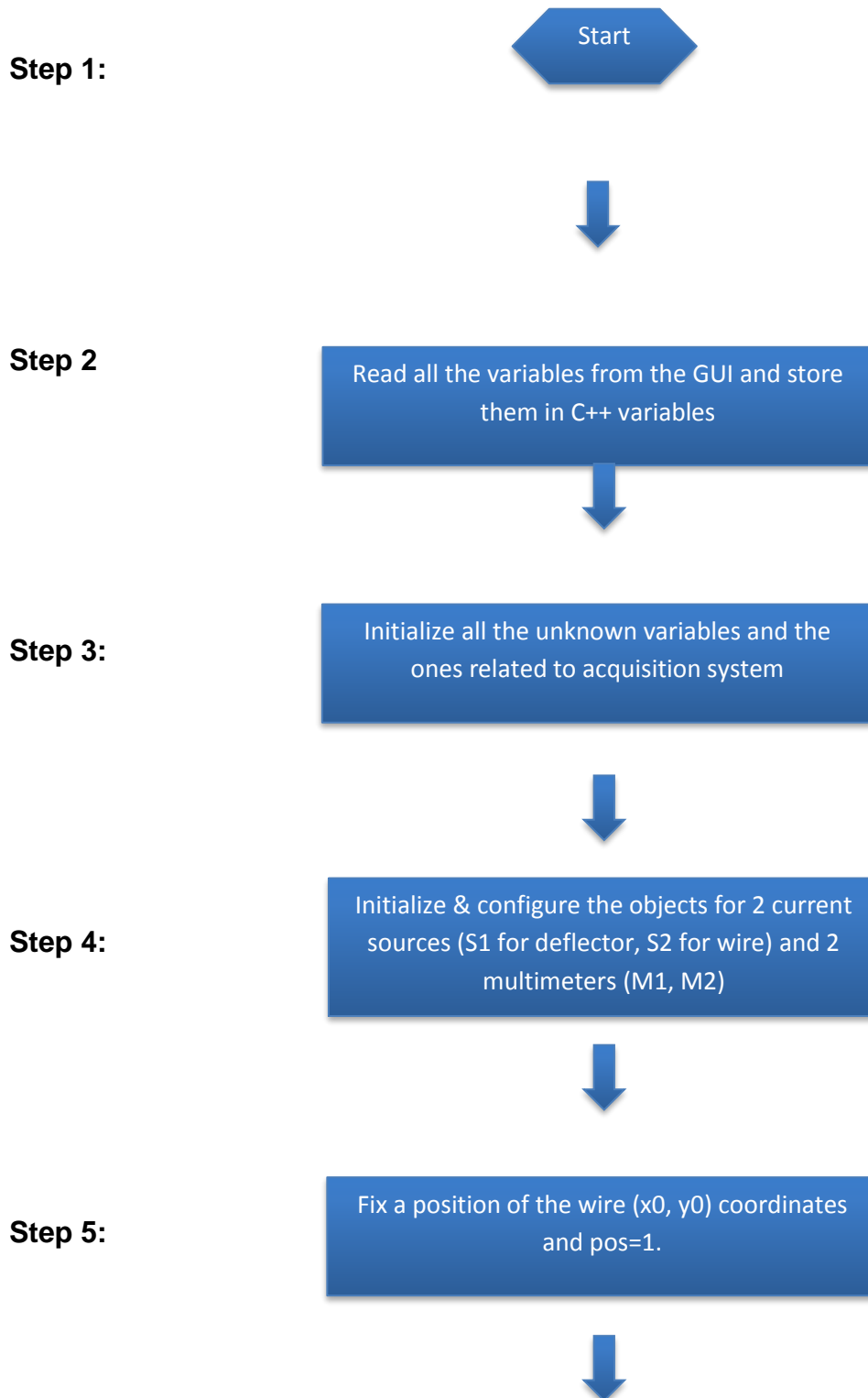
The advantage of using the C++ script was that the drivers of all the hardware (used for acquisition and wire displacement) were available and were implemented on the magnetic measurement test bench. Some minor changes to the drivers were done which include adding some functions e.g. compliance function for Keithley current generators and the phase marker setup for synchronization of the current generators.

An existing GUI script which was used for magnetic measurements was modified accordingly for the data which is required to be input for the stretched field measurement.

For every single measurement, it takes almost 0.5-1 hour to produce the result depending on the selection of the grid and number of points to be measured. The scripting took most of the time of the thesis but due to the copy right issues of CERN, the scripts cannot be included with this report.

A complete algorithm which was designed for the measurement is explained in the following sections.

The following block diagram explains the C++ script:



Step 6:

Iterate on the values of the amplitude of S2 starting from the minimum value.



Step 7:

Measure across the shunt resistor through M1 and across the deflector plates using M2.



Step 8:

Write the following files: Parameters.txt for all the given parameters e.g. deflector & wire voltage, Positions file Ax_Ay_Bx_By_kHz_defl.voltageV.txt, Acquired data file through M1 & M2 in X_xposition_Y_yposition_wire-

Change the amplitude of S2 by a given fixed value and move to step 7

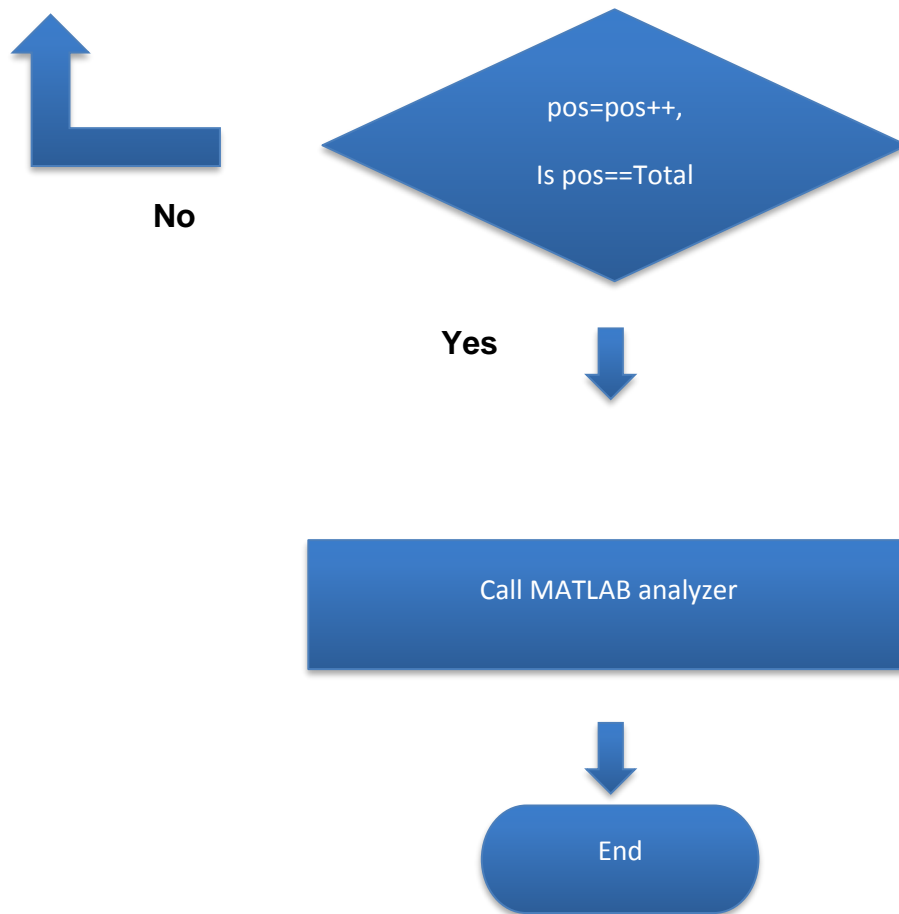


No

Change the position of the wire to a new coordinate and move to step 6

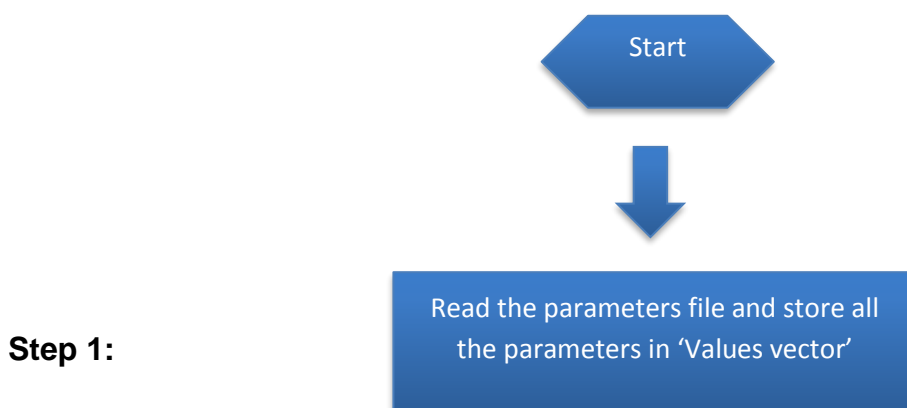
Yes





8.2 Analysis in MATLAB

MATLAB is used for final analysis. The algorithm used is to read the data from all the files and import it to variables in MATLAB. Following flow chart explains the step by step process:





Step 2:

Read the position files and store position values in Xpos and Ypos.



Step 3:

Read the rms values of wire voltages and deflector voltages for a fixed position.



Step 4:

Using the rms values of wire voltages against the applied current through S2, fit a curve. Plot the data points both for fitted and nonfitted points. Find the minimum and store it.



Go to the next set of files on step 3

No

Is minimum for each position obtained?

Yes

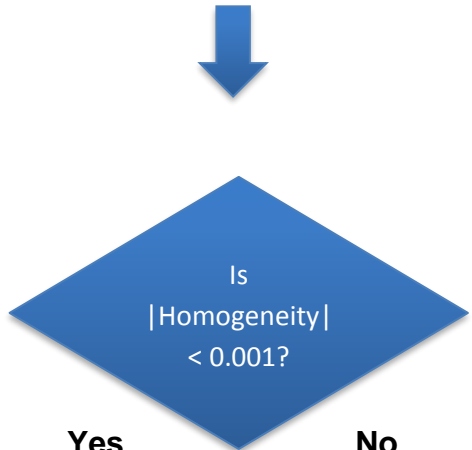


Step 5:

Using the minimum voltage of each position, the corresponding value of S2 amplitude is used from the fitted values and electric field profile is generated by using equation $E = -dV/dx$

Step 6:

Now taking the Electric field value at the position (0,0) as reference, evaluate Homogeneity= $1-E/\text{Reference}$.

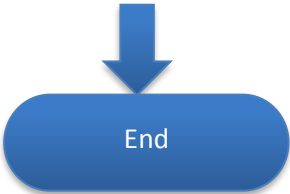


Step 7:



Step 8:

Draw the deflector and plot the corresponding Homogeneity points as *



8.3 Final images of the setup before the first measurement

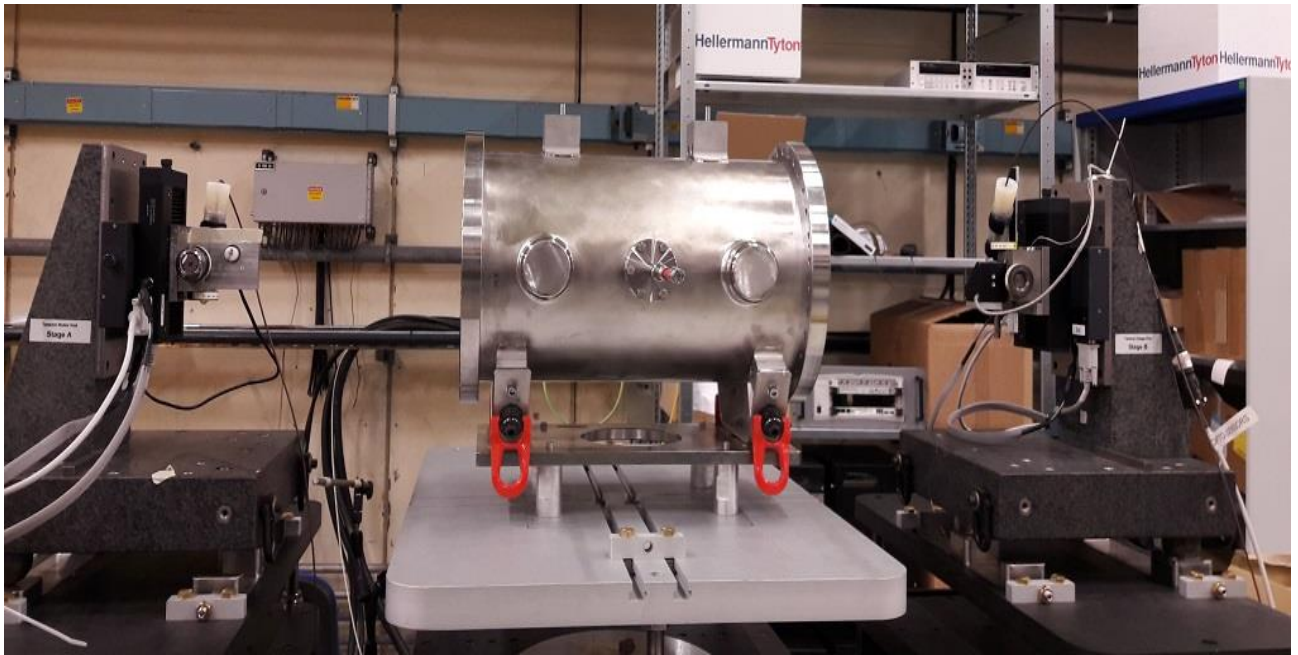


Figure 52.

The above figure shows the final assembly of the deflector mounted on the test bench with stretched wire and both ends of the wire are tied to the positioning stages which can move along x and y axis up to 10 mm each with as small as a step of $1\mu\text{m}$.

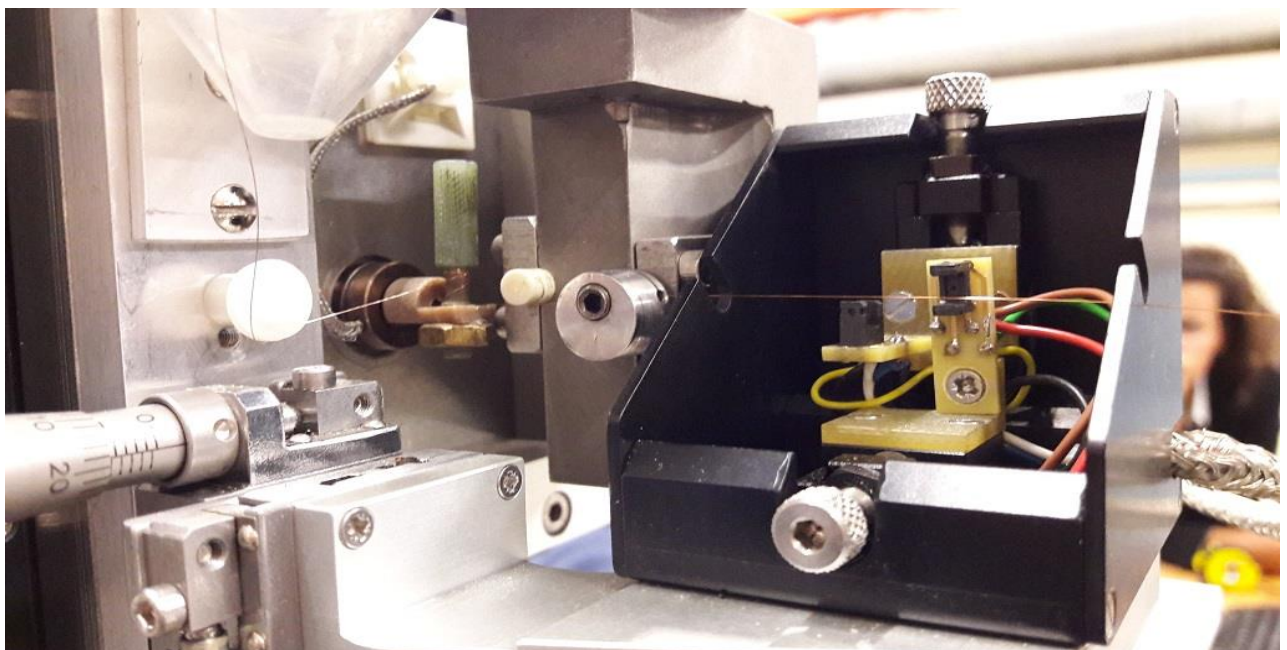


Figure. 53

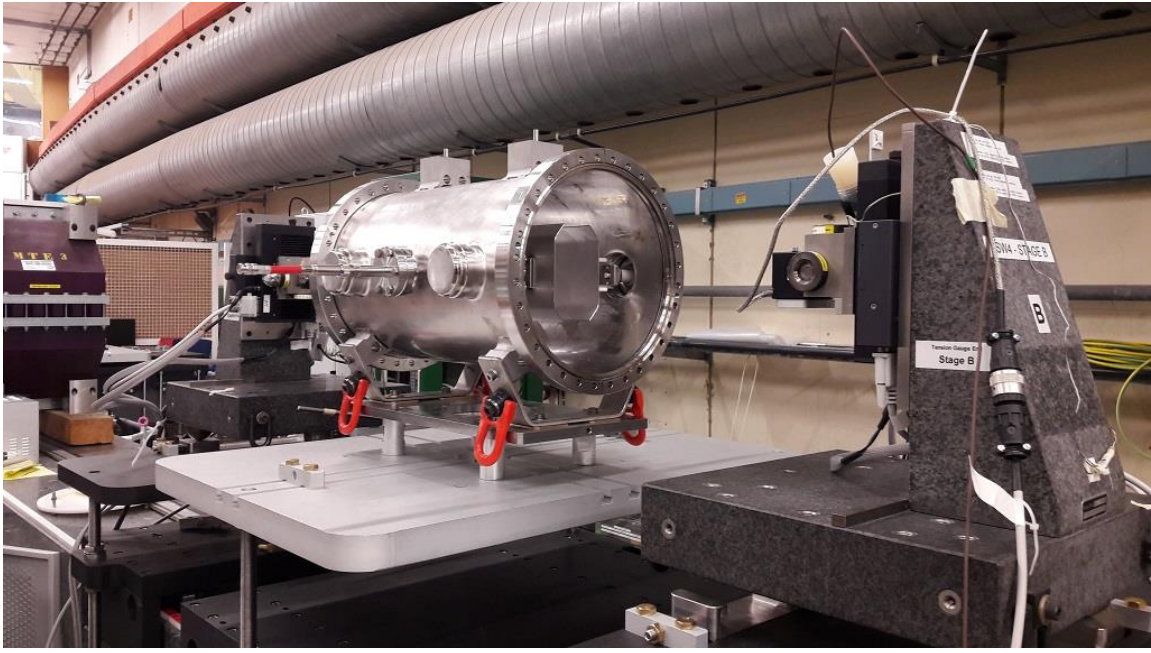


Figure. 54



Figure. 55

8.4 Functioning of the test bench

The test bench is started by running the C++ script.

Step 1: Run the program Electric field measurement & select *Stretched wire for Electric Field*

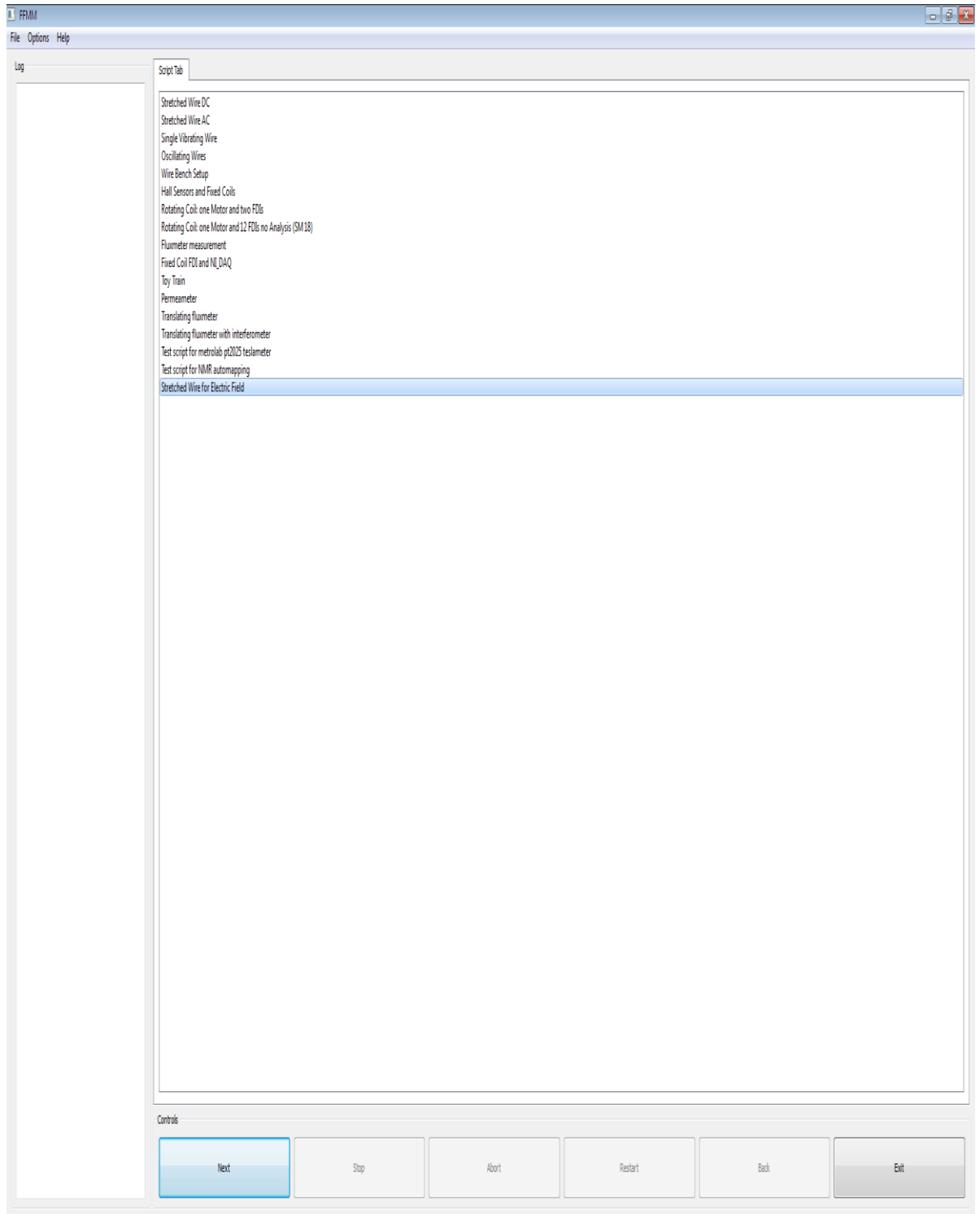


Figure 56.

Step 2: Enter deflector voltage, wire voltage (steps, minimum & maximum values), positions

The screenshot displays the 'Stretched Wire for Electric Field' software interface. The window is divided into several sections for configuration:

- File:** Operator name: khuram; Output directory: C:\Measurements\EFieldTest
- Bench:** SWI system number: 4; Move stages position before measurement; Move to reference Position when starting
- Wire tension:** Wire tension; Maximum wire tension: 650.0 [g]
- Wire Voltage:** Wire Voltage; Frequency: 4000 [kHz]; Minimum Value: 0.6 [V]; Maximum Value: 1.9 [V]; Number of amplitude values: 10
- Deflector Voltage:** Deflector Voltage; Amplitude value: 8 [V]
- Measurement:** Number of measurement repetitions: 1; Stop procedure between wire displacements; Show analysed plots; Correction of the wire position after the measurement; Maximum adjustment: 0.0 [mm]
- Deflector Info:** Deflector Name: []; Deflector width: 50.0 [mm]; Deflector height: 80.0 [mm]
- Wire Trajectory:** Trajectory roll angle: 0.0 [deg]; Counter-directional; Direction: Select: Grid; X Semi-Displacement: 1 [mm]; Y Semi-Displacement: 1 [mm]; Number of acquired Points in X: 7; Number of acquired Points in Y: 7

At the bottom, there is a 'Controls' section with buttons for Next, Stop, Abort, Restart, Back, and Exit.

Figure 57.

In the above figure, the window contains the name of the person starting out the measurements and the path of the measurement files to be written. For the bench settings, it asks you which test bench you are operating on, this is just a protocol to be followed in the laboratory. We can also select if we like to move the stages before measurement and to move at the reference position in the middle of the deflector. Then we can select the frequency of the wire voltage signal, minimum and maximum voltage to be applied to the wire with number of steps of the sweep to be taken.

Deflector voltage amplitude is set as well. Moreover, if we like we can repeat the measurements more than one time but it has been chosen once to save time. Deflector dimensions are important to mention since it will allow to model the grid of measurement. The positions at which measurements should be taken from left to the right and top to the

bottom are determined by putting X and Y displacement coordinates and number of points to be taken from -X to X with each fixed value of Y coordinate from -Y to Y.

Step 3: Align the wire to the center of the deflector automatically

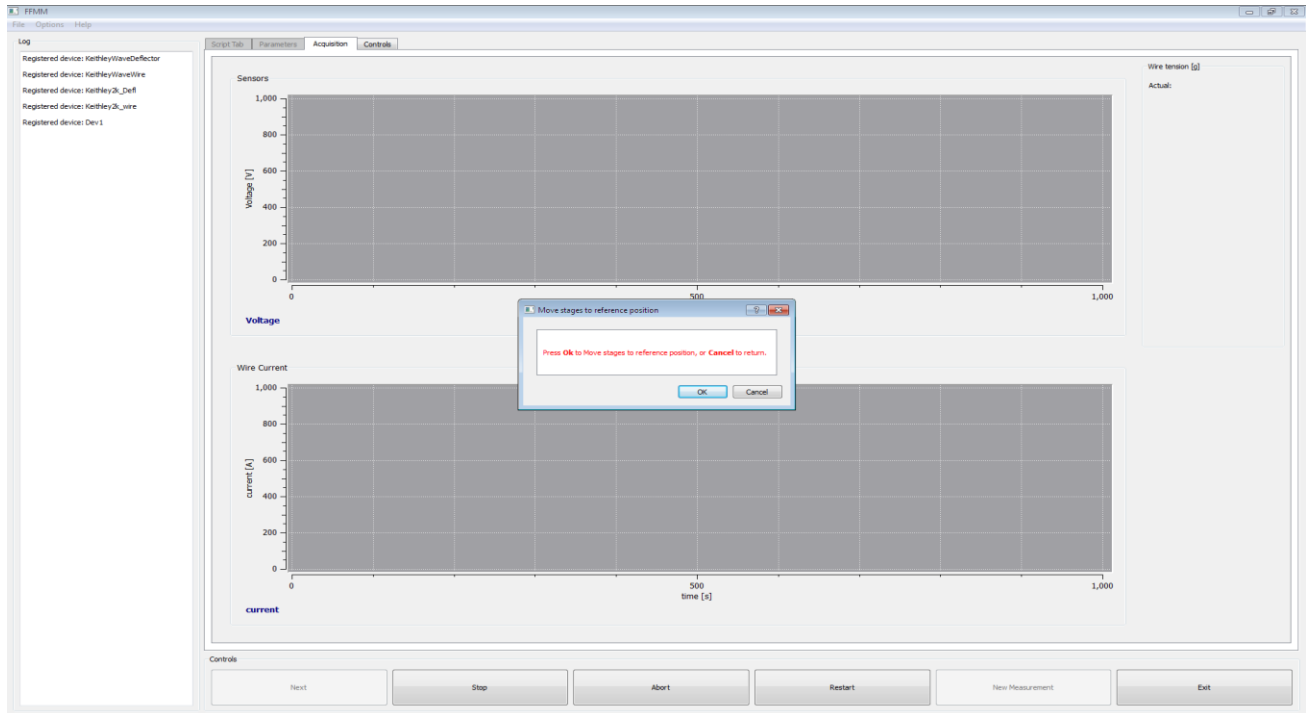


Figure 58.

In the above figure, the test bench asks to confirm to move the stages of the at reference position (0,0) for a grid of (-10 mm, -10 mm) to (+10 mm, +10 mm) .

Step 4: Manually adjust the position if needed

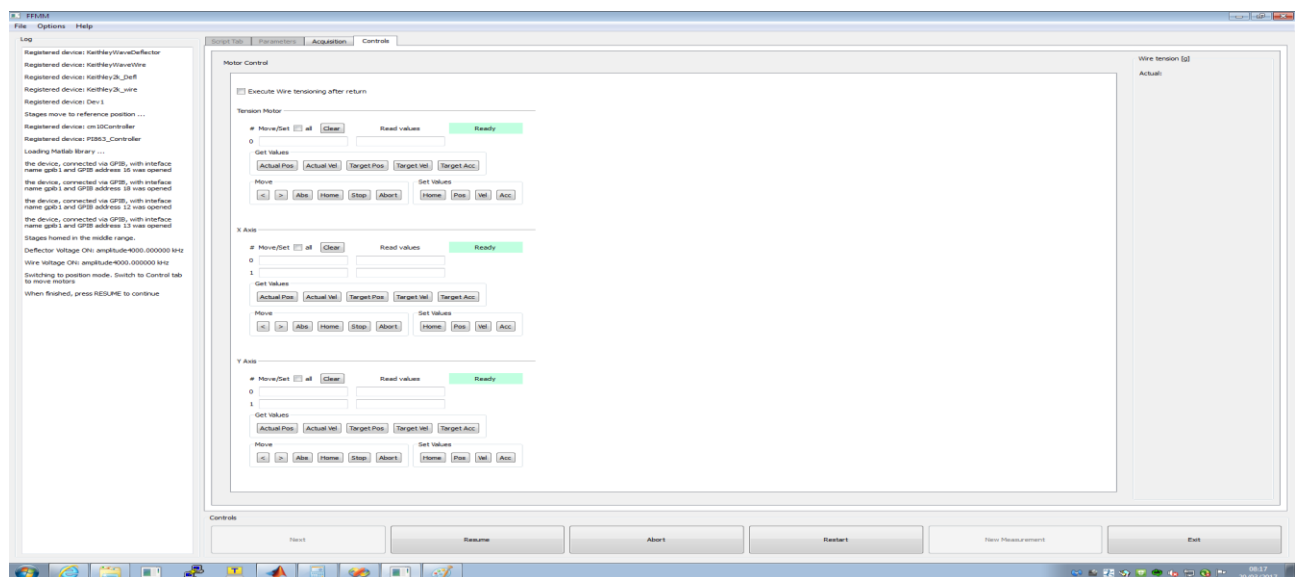


Figure 59.

Step 5: Start measurement

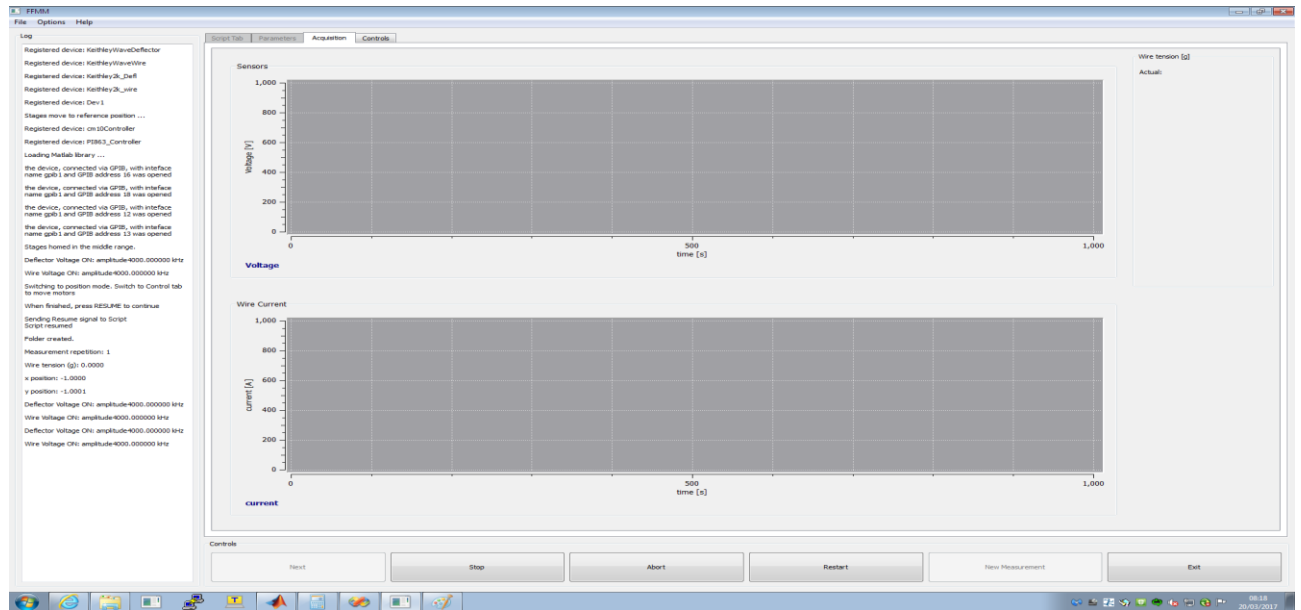


Figure 60.

The measurement process takes almost 0.5 to 1 hour for evaluation of electric field for a specified grid. For each fixed point (x, y) position coordinate, the applied current makes a sweep and then for each value of the sweep the system is reset so that the measurement is synchronized. Although still the till delay in the measurement is around $0.1 \mu\text{s}$ with our signal period is $250 \mu\text{s}$ which is around 0.04%.

Step 6: First plot appears of fitted data and data points.

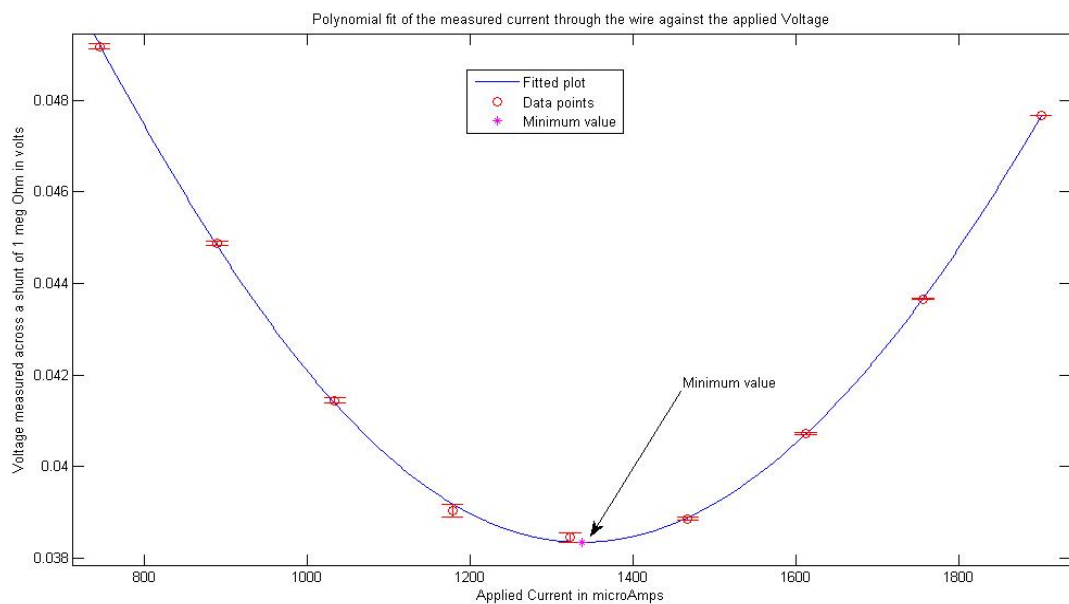


Figure 61.

In the figure, the circles show the exact measurement points and continuous line shows the fitted plot. The graph shows that at the origin ($x=0, y=0$) which is exactly in the middle of the deflector, the induced charged is minimized by applying the increasing value of current through the current source. At first the voltage measured by the voltmeter connected to the wire through the ground is high and as soon as the applied voltage tries to balance the induced charge, it goes down by reaching to the minimum and then rising again in the other direction. The curve is fitted with 7th degree polynomial using the MATLAB function of curve fitting.

$$p = \text{polyfit}(xdata, ydata, n) \tag{22}$$

where the function *polyfit* takes variables of *xdata* and *ydata* from the measurement data. The *n* denotes the number of degree of the polynomial for the fit, the number is chosen with the approximation that the curve is assumed to follow the pattern of almost a parabolic distribution. The output of the function is the coefficient of the fitted curve polynomial which is then used to get the continuous values of the voltage curve points through the whole range of applied current.

$$y_fit_value = \text{polyval}(p, xdata_wholerange) \tag{23}$$

The plot also displays the error bars in the measured value which is in accordance to the uncertainty in the voltage measurement of the multimeter.

$$\text{Uncertainty in Voltage measuerment} = 0.008 \% \tag{24}$$

Step 7: Electric Field plot appears for a fixed y position

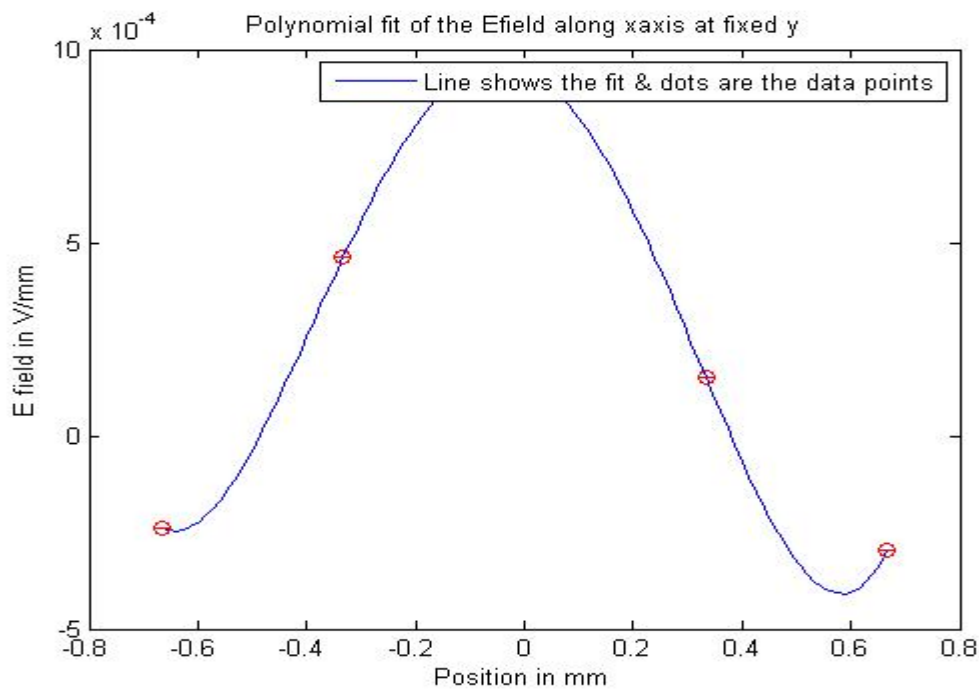


Figure 62.

The plot in figure 62. shows the absolute values of the electric field measured at $y=0$ position along the x -axis. Red circles show the measured points and the continuous curve is the fitted curve using the calculated points from the measured data. The curve fitting is done again using the same equation (23) and (24). The measured electric field is in the range of the order of 10^{-4} and the variation is expected to lie in the same region as well.

The plot also contains the total error in the calculated electric field which is explained by the following equations:

$$\% \text{ Error in } E. \text{ field} = \% \text{ Error in Voltmeter} + \% \text{ Error in position} + \% \text{ Error due to synchronization} \quad (25)$$

$$\text{Required uncertainty in the measurement} < 0.1\% \quad (26)$$

$$\text{Required uncertainty in position} < 0.05\% \quad (27)$$

$$\text{Total uncertainty in } E. \text{ field} = 0.098\% < 0.1\% \quad (28)$$

Hence, the measured results are still under the required tolerance level but still it is very close to the target uncertainty.

Step 8: Final plots.

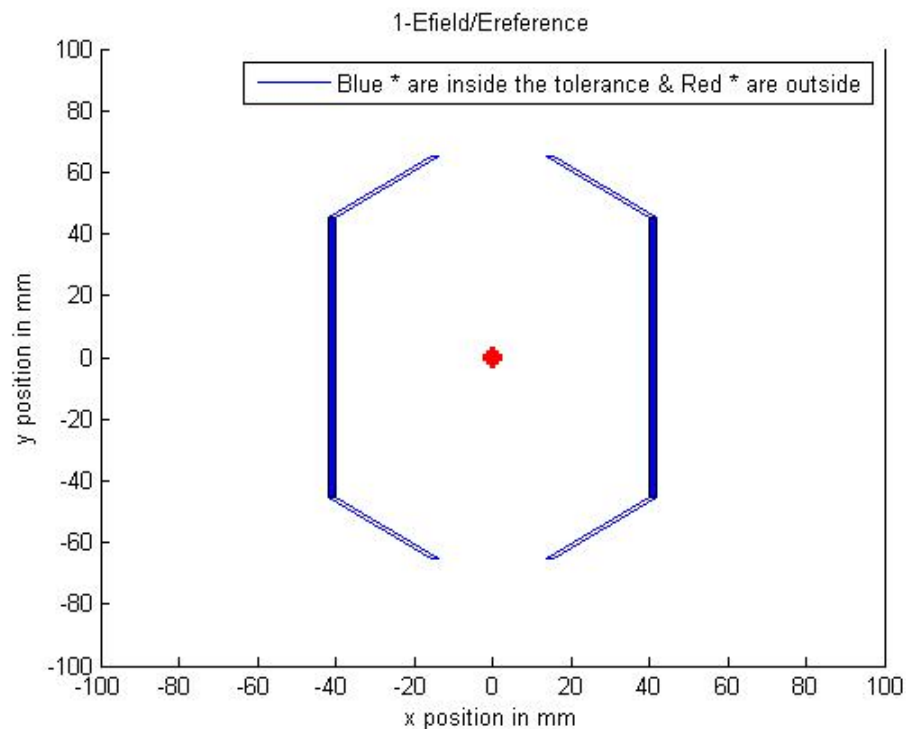


Figure 63.

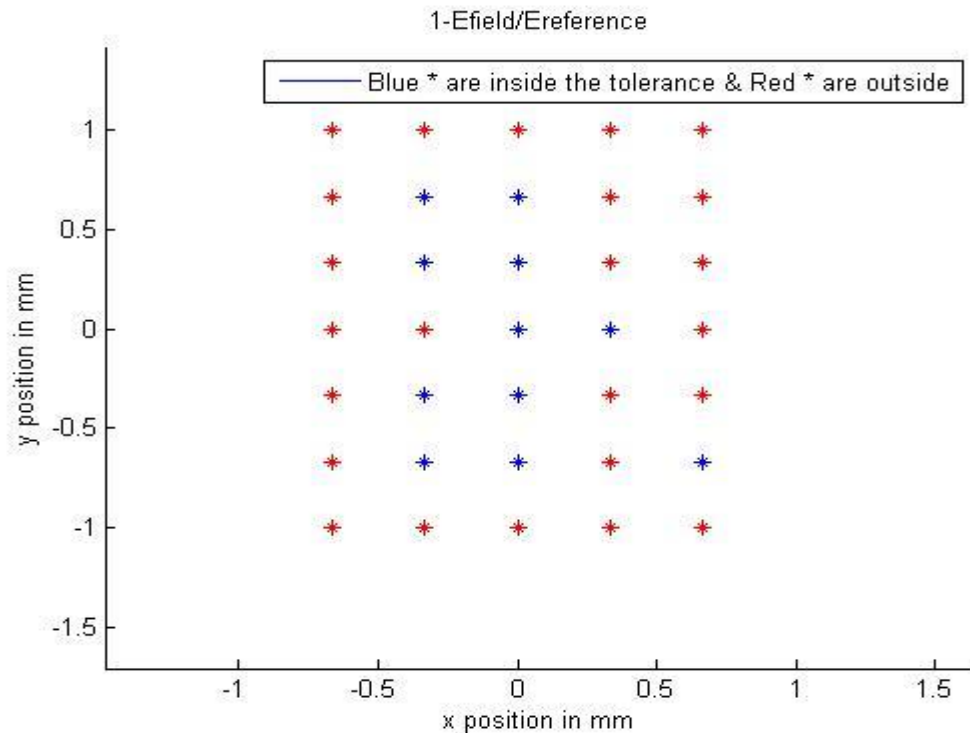


Figure 64.

The above plot shows the points with blue and red asterisk. Blue asterisks are the points which are under the tolerance of field variation factor of 0.001 with respect to the reference value. Although, there are some abnormalities being observed since near (0.6 mm, -0.6 mm) a blue asterisk is observed and its surrounding contains red asterisks. This is most probably because of an error in the measurement in accordance to the equations (25), (26), (27) and (28).

The blue dots along the y axis for a fixed axis position verify that the field is homogeneous along the y-axis which follows the theoretical results since the field is varying only along the x-axis. Since the deflector plates are not 100% symmetrical, the result shows antisymmetric field homogeneity. The points are symmetric along the y-axis with respect to the origin but the symmetry is lost along the x-axis. This can be due to the tilt of one of the plates of deflector. Although, with the help of more experimental data evidence it can be observed that whether if it's an effect of tilt or not.

The measured region of field homogeneity comes out to be lying between -0.5 mm to 0.5 mm as compared to the simulation models of COMSOL where it was between ± 4 mm from center. This huge difference needs more research so that the measurement should get closer to the simulation model.

8.5 Conclusion

Measurement of electric field homogeneity up to such a low variation factor of 0.001 is a challenge. But the results show that in a certain range around the center such region exists and further investigation is required why the region is smaller than the one that appeared in the simulation. The existing setup is still good enough for such a precise variation measurement.

8.5.1 Possible errors

- **Alignment of the deflector plates with respect to each other:**

The plates facing each other must be perfectly parallel to each other, this can lead to change in the electric field profile homogeneity. This alignment can change the effective surface area facing the wire of both the plates. As a result, the capacitance between the wire and the plates do not remain uniform. Electric field homogeneity shifts along with the angle. The error in this case can be more than 0.1 % which is above the tolerance level.

- **Alignment of the wire:**

The wire should also be positioned parallel to the plates otherwise the equipotential will not be achieved which is highly possible in our case where the measured voltage of the current through the wire does not reach to zero.

- **Generators are not 100% synchronized:**

Frequency difference of less than 1 mHz exist. The best way to solve this problem is to use a lone source and then wire potential is changed using a motorized potentiometer. This error is a possible cause that the voltage does not go below 38 mV. Moreover, the delay in the measurement because of the synchronous measurement issue adds 0.04% error which should be further reduced.

- **Voltage on the plates:**

Voltage is not fixed up to 4th precision digit during the motion of wire from one position to the other. A constant voltage source is required so that the voltage difference on the plates remains constant or must not vary by 0.01%.

8.5.2 Challenges faced

- **Measurement of the capacitance of the deflector:**

The measurement of a very low capacitance was a challenge since the measurement setup should be carefully chosen so that the measurement system capacitance must be lower than that of deflector.

- **Phase shift:**

One of the reasons that may have caused the current through the wire not reaching minimum is phase shift. This phase shift occurred because of the alignment problems and mainly because of the impedance of multimeter used. (Ideally it should be very high of the order of giga ohms).

- **Synchronization of Generators:**

Synchronization of both generators was a big challenge. An option in the Keithley current generator allowed to send a pulse of 0.1 us to the second generator to start the generation. But this pulse is sent when the first generator reached the phase angle of 180 degrees to compensate the delay of 0.1 us. Moreover, the frequencies of the generators were not completely synched and there was a difference of less than 1 mHz because of difference of clocks in each generator.

- **Limitation with the DAQ used NI 6289:**

Initially NI 6289 was used to acquire all the measurements, but it showed a strange behavior. As the DAQ sampled the signal to take the measurement, it destroyed the original signal. The probable causes were the leakage of the measurement signal to the ground through the input capacitance of DAQ.

8.5.3 Future recommendations

- Use of one source is recommended highly or sources which can share the same clock. This can eliminate the errors regarding the synchronization issues.
- The voltage source must be improved so that the voltage on the plates must not change more than by 0.0001 V.

- Analog motorized potentiometer with a feedback control of position can be used to involve a motorized control using a potentiometer leading back to the original approach.
- Measurement should be carried out in a metallic enclosed tank so that the surrounding fields do not interact with the measurement.
- A similar approach can be used to position the plates to deflect the beam in the vertical direction by installing another set of plates at 90 degrees to both plates. This will require that first the homogeneity issues along the x-axis is solved.

Bibliography for References

- [1] Cern website: <http://home.cern/>

- [2] Alexander B. Temnykhy and James J. Welch, Wilson Laboratory, Cornell University, Ithaca NY, "Improved methods of Electric Field Uniformity in an Electrostatic Separators," [Online]. <http://ieeexplore.ieee.org/stamp/stamp.jsp?tp=&arnumber=505480>.

- [3] ELENA Fast Coupled deflector Reference manual **LNA-ZDFA-ES-0001**.

- [4] CONCEPT FOR ELENA EXTRACTION AND BEAM TRANSFER ELEMENTS
<https://cds.cern.ch/record/1574727/files/CERN-ACC-2013-0082.pdf>
<https://www.monroe-electronics.com>

- [5] Measurement of Electric Field by Weiran Lou and James. J.Welch Cornell University
https://www.classe.cornell.edu/public/CBN/1995/CBN95-7/cbn95_7.pdf

- [6] LHC MTA SSW Report.

- [7] INA118 datasheet by Texas Instruments

- [8] Fluke Scope Meter 1900 series reference manual

- [9] Keithley 2000 Multimeter user manual

- [10] National Instruments PXIe 1071 reference manual

- [11] National Instruments PXIe 8100 reference manual

- [12] National Instruments PXIe 4081 reference manual

- [13] National Instruments NI 9260 reference manual

- [14] Keithley 6221 Current Generator user manual

- [15] ELENA drawings from CERN EDMS

- [16] LHC Test Procedure SSW for SSS from CERN EDMS

- [17] MONROE Electronics a review of current methods to measure electric field

